Quantifying the Effects of Sea Level Rise on Estuarine Drainage Systems

K. Waddington[1], D. Khojasteh[1], L. Marshall[2] , D. Rayner[1] and W. Glamore[1]

[1] Water Research Laboratory, School of Civil and Environmental Engineering, UNSW Sydney, NSW 2093, Australia.[2] Water Research Centre, School of Civil and Environmental Engineering, UNSW Sydney, NSW 2052, Australia.

Corresponding author: Katrina Waddington (k.waddington@unsw.edu.au)

Key Points:

- The *drainage window* is conceptualised and applied to two estuaries to quantify the effects of sea level rise on tidal drainage systems.
- Areas that are protected from intermittent flooding may be vulnerable to chronic waterlogging due to impeded drainage.
- Loss of function and amenity due to impeded drainage should be considered in future land use planning.

Abstract

Much of the development of the low elevation coastal zone has involved the reclamation of low-lying floodplains and wetlands through the construction of flood mitigation and drainage systems. These systems function throughout the tidal range, protecting from high tides while draining excess catchment flows to the low tide. However, drainage can only be achieved under gravity when water levels in the catchment drains are higher than those in the estuary. Changes to the tidal range and to the duration of the rising and falling tides that occur throughout estuarine waters will result in dynamic variations in the window of opportunity for gravity discharge within and between different catchments and under sea level rise (SLR). Existing concerns regarding SLR impacts have focussed on the acute effects of higher water levels, but SLR will affect the full tidal range, and drainage systems will be particularly vulnerable to changes in the low tide. This study introduces the concept of the *drainage window* to address this limitation by assessing how the present-day and future SLR tidal regimes may influence the drainage of different estuarine floodplains. Applying the drainage window to two different estuaries indicated that SLR may substantially reduce the opportunity for discharging many estuarine floodplain drainage systems. Reduced drainage creates a host of chronic problems that may necessitate changes to existing land uses. A holistic assessment of future changes to all water levels (including low tide levels and extended flood recession periods) is required to inform strategic land use planning and estuarine management.

Plain Language Summary

Estuaries are the tidal waters located where rivers meet the sea. The floodplains adjacent to estuaries are some of the most heavily developed areas in the world. Much of this development relies on integrated flood management and drainage schemes that use one-way valves (floodgates) to protect the floodplains from inundation by high tides and floods, while allowing the floodplain drains to discharge when the water level in the estuary is lower than the water level in the drains. Tidal levels can vary along an estuary and may change under accelerating sea level rise (SLR). This study introduces the concept of the *drainage window* to quantify how much time is available to drain different floodplain catchments within an estuary and to identify how that window of opportunity may be affected by SLR. The drainage window was analysed for two estuaries, with the results indicating that SLR may substantially reduce the time available to drain each system. Areas with less time to drain are more susceptible to chronic problems associated with prolonged inundation and waterlogging that may necessitate changes to existing land uses. These results could therefore be used to inform strategic land use planning and management in estuaries worldwide.

1 Introduction

As the nexus between land and sea, coasts and estuaries have been a focal point for human settlement, with their abundance of natural resources and ecosystem services attracting extensive and ongoing development (Martínez et al., 2007; Neumann B, 2015). Worldwide, over one billion people reside less than ten metres above current high tide levels (Domingues, Santos, de Jesus, & Ferreira, 2018; Kulp & Strauss, 2019). Two-thirds of the world's megacities are situated on coasts and estuaries (Oliver-Smith, 2009) and approximately 14% of the world's gross domestic product is generated in the low elevation coastal zone (Magnan et al., 2019).

Much of the development of the low elevation coastal zone has been facilitated by the anthropogenic drainage of floodplains and wetlands, predominantly for agriculture, but also for urban, maritime, and industrial use (Church, Woodworth, Aarup, & Wilson, 2010; James G Titus et al., 1987; Tulau, 2011). Channels, pipes and culverts have been installed throughout estuarine catchments to efficiently remove excess surface and groundwater from backswamps, wetlands, and floodplains (J. G. Titus et al., 2009). Frequently, natural levees are augmented and dykes and seawalls are constructed to protect these lands from tidal inundation or high fluvial water levels (Kroon & Ansell, 2006; Lugo & Snedaker, 1974; Poulter, Goodall, & Halpin, 2008). The reclaimed areas created by these works are variously referred to as polders, *koogs*, or *wei*. Intermittently operated tidal gates, such as the Thames Barrier in London (Horner, 1979) or the Lake Borgne Surge Barrier in New Orleans (Huntsman, 2011) may be used to prevent storm surges from progressing upstream along an estuary. To protect low-lying floodplains and reclaimed lands from regular inundation by high tides however, one-way valves (herein referred to as floodgates, but also known *inter alia* as tidal flaps, flap gates, non-return or reflux valves) are often installed where tributaries or drainage channels discharge to the main estuary (Johnston, Slavich, & Hirst, 2005; Ota, 2018; Ruprecht, Glamore, & Rayner, 2018). Tidal floodgates are widely implemented throughout estuaries along the east coast of Australia (Boys, Kroon, Glasby, & Wilkinson, 2012; Williams & Watford, 1997), and can also be seen in Europe (Díez-Minguito, Baquerizo, Ortega-Sánchez, Navarro, & Losada, 2012; Solomon, 2010), Asia (Award, 1995; Choi, 2014; Warner, van Staveren, & van Tatenhove, 2018; Zhao et al., 2020), and North America (Giannico & Souder, 2004; Rillahan, Alcott, Castro-Santos, & He, 2021). These floodgates operate throughout the full tidal range, providing protection against high tide inundation while facilitating drainage to the low tide level. Their continued operation will therefore be vulnerable to future sea level rise (SLR).

Globally, the impacts of SLR are already being experienced in the low elevation coastal zone (Magnan et al., 2019), with the largest changes in tidal dynamics observed in estuaries and tidal rivers (Talke & Jay, 2020). According to the latest report from the Intergovernmental Panel on Climate Change (IPCC), the average global mean sea level is predicted to increase by between 0.28 m and 1.01 m by 2100, relative to 1995-2014 average (Masson-Delmotte et al., 2021). A growing body of literature indicates that, within estuaries, the impact of SLR will vary throughout the full tidal range, with diverse effects from high to low tide levels (Haigh et al., 2020; Khojasteh, Glamore, Heimhuber, & Felder, 2021; Talke & Jay, 2020). Each estuary, including tributaries and different reaches within an estuary, may respond differently to SLR (Du et al., 2018; Khojasteh, Chen, Felder, Heimhuber, & Glamore, 2021).

While the potential for reduced drainage due to higher low tide levels has been recognised (Khojasteh, Glamore, et al., 2021), the implications of changing tidal dynamics on floodplain drainage have received limited attention and are yet to be quantified. Despite the experience of low-lying areas in the Netherlands (Hoeksema, 2007) and Indonesia (Wahyudi et al., 2019), for example, where excess surface and groundwater must be pumped to the receiving waters, inundation due to SLR has been regarded as a consequence of higher peak sea levels (Holleman & Stacey, 2014) rather than a lack of drainage. Consequently, the majority of research has focused on the potential impacts of SLR on the extent and frequency of extreme coastal storms and flooding (Bosello & De Cian, 2014; Vitousek et al., 2017), groundwater emergence (Hoover, Odigie, Swarzenski, & Barnard, 2017; Manda, Owers, & Allen, 2017; Wake et al., 2019) and increased nuisance ("sunny day") flooding (B. S. Hague, McGregor, Murphy, Reef, & Jones, 2020; Hanslow, Fitzhenry, Power, Kinsela, & Hughes, 2019; Karegar, Dixon, Malservisi, Kusche, & Engelhart, 2017). Yet drainage infrastructure is crucial for the effective management of these intermittent events. Indeed, in urban and industrial environments, constructed drainage systems are primarily designed to mitigate flood risk (ASCE, 1992), although they play a critical role in maintaining public health and amenity (Barbosa, Fernandes, & David, 2012; Gaffield, Goo, Richards, & Jackson, 2003; Vlotman, Smedema, & Rycroft, 2020) and optimising agricultural productivity (Cavazza & Pisa, 1988; Hurst, Thorburn, Lockington, & Bristow, 2004).

A typical floodplain drainage scheme consists of a series of interconnected open channels or piped culverts which allow surface and groundwater to drain under gravity and ultimately discharge into the adjacent waterway. Floodgates preclude the flow of tidal waters from the estuary to the floodplain, only permitting discharge from the floodplain catchments when sufficient positive hydraulic head is provided, i.e. when water levels in the catchment drains are higher than those in the estuary (Giannico & Souder, 2004). At any point within an estuary, the availability of a positive hydraulic head is influenced by the catchment runoff and hydraulic characteristics of the drainage system upstream of the floodgates and the tidal water elevation downstream of the floodgates. The tidal water levels are characterised by the amplitude (tidal range) and shape (tidal duration asymmetry) of the tidal wave, which may be distorted by the effects of friction, convergence, reflection and inertia (van Rijn, 2011) and is subject to changes to the geometry of an estuary. Additionally, SLR has the potential to modify the water depth, width convergence, floodplain connectivity or entrance conditions of an estuary, which, in turn, can affect the propagation of tidal waves along an estuary (Haigh et al., 2020; Khojasteh, Glamore, et al., 2021; Talke & Jay, 2020). Any changes to the tidal water levels and/or duration can influence the time available for drainage of the estuarine catchments, which may have significant impacts on the estuarine environment, including current land use and management.

To assess how the tidal regime may influence the drainage of estuarine floodplains, and particularly the potential impact of changing tidal regimes under SLR, this study introduces the concept of the *drainage window.* The drainage window describes the relationship between hydraulic head and the time available for the gravity discharge of floodplain catchments based on local tide characteristics. The drainage window is calculated and applied at two different estuaries in south-east Australia to highlight how SLR may affect floodplain drainage. The influence of present-day and future SLR hydrodynamic regimes on the drainage window is discussed in relation to reduced catchment drainage and potential impacts on existing land management practices.

2 Methodology

2.1 Defining the drainage window

Within coastal and estuarine drainage systems, the drainage window is the portion of the tidal cycle when a positive hydraulic head is available to facilitate gravity discharge to the receiving waters at a selected elevation (Figure 1). This describes the temporal period provided both by the tide (at a nominated water level) and to the drainage catchment (at the same topographic level). Under wet weather and flood conditions, the drainage window will vary dynamically, with differential water levels between the estuary and floodplain drainage system subject to local and regional rainfall distribution and the diverse hydrologic and hydraulic responses of catchments throughout both the estuary and upstream river system. Conversely, during non-flood, or dry weather periods, and in the absence of any significant catchment or river inflows that may otherwise affect the hydraulic gradient between the drainage channels and estuary, the drainage window at a given site is primarily controlled by daily tidal conditions. Floodplain drainage systems typically include numerous minor and high-level outlets located above or within the upper portion of the tidal range, in which case the drainage window will also be affected by the invert level of the outlet. However, throughout the lower lying floodplain areas, the primary floodgates servicing the main drainage systems are located at or below the lowest tidal levels to maximise the opportunity for discharge (Ruprecht et al., 2018). Thus, as indicated in Figure 1(a), the drainage window would be restricted to the falling tide, with floodgates precluding discharge as a negative hydraulic gradient develops during the rising tide. In these circumstances, the drainage window can be simply defined as the height above the low tide. Thus, assessing the drainage window at the low-lying floodgates under dry weather conditions provides a benchmark to identify the relative opportunity for flows from different floodplain catchments to discharge to the low tide, with increased potential for waterlogging and prolonged inundation to develop when drainage is persistently limited.

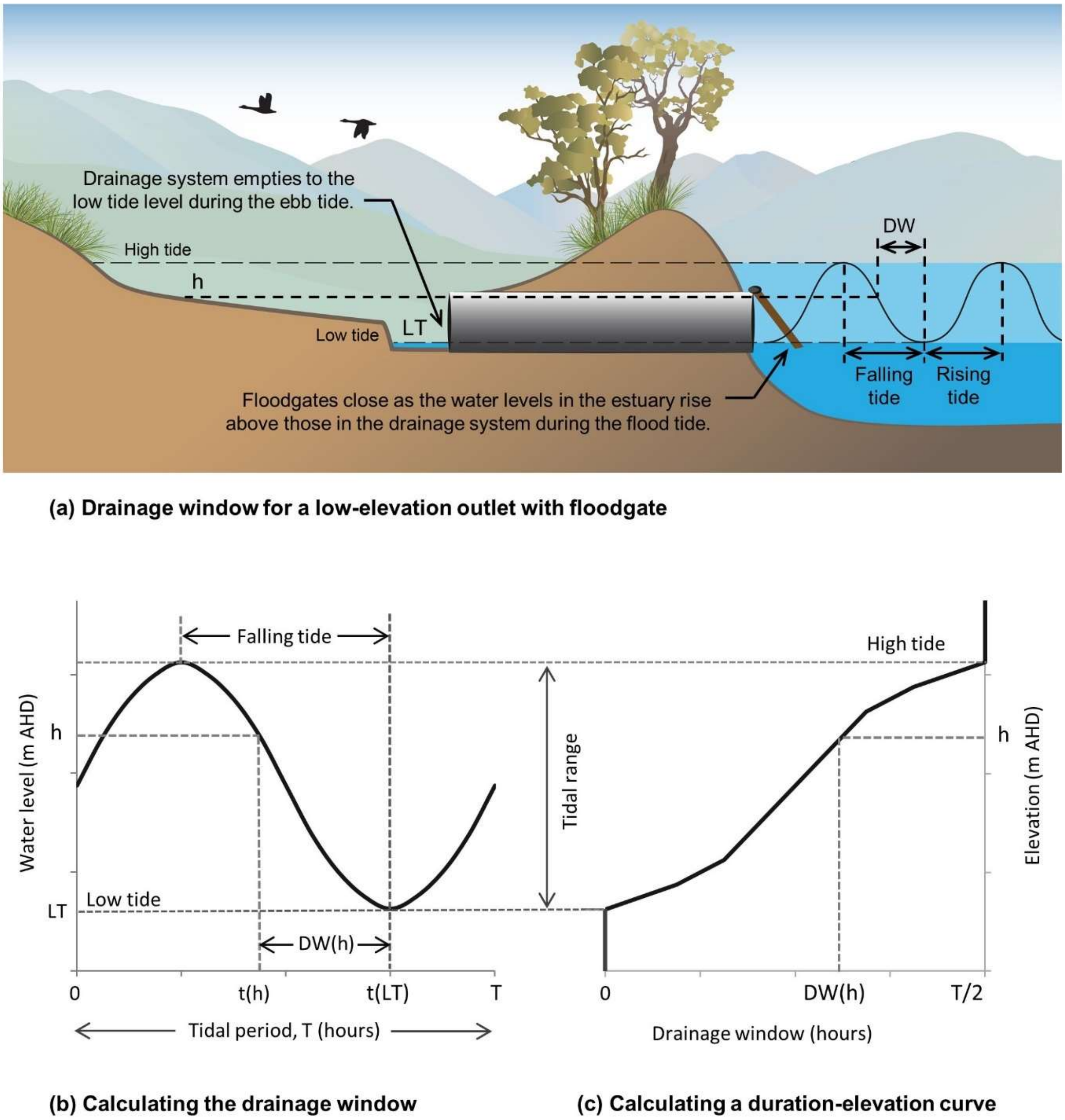

Figure 1 (a) Graphic representation and (b) mathematical definition of the drainage window (DW) for a low-lying floodgate (invert level at or below low tide). During dry weather, discharge is precluded during the rising tide as increasing water levels in the estuary close the tidal floodgate, limiting the drainage window to the time available to discharge from a nominated elevation, h, to the low tide level, LT. The duration-elevation curve for the drainage window (c) is developed by calculating the drainage window at regular intervals over the full tidal range.

As illustrated in Figure 1(b), for a nominated elevation (*h*), the drainage window for a single tidal period (DW_h) is a function of the time (*t*) it takes for the tide to fall from the same water level (*h*) to the low tide level (*LT*):

$$DW_h = t(h) - t(LT) \geq 0 \quad (1)$$

When calculated incrementally over the full tidal range, the results can be graphed as a drainage window duration-elevation curve (conceptualised in Figure 1(c)) representing drainage conditions specific to each floodgate. The elevation axis of the drainage window duration-elevation curve can then be compared to topographic levels (using a hypsometric curve and mapping as described in Section 2.5) to identify areas vulnerable to reduced drainage. This technique may be equally applied to identify critical levels and to assess storage capacity within drainage infrastructure.

The drainage window duration-elevation curve may vary throughout an estuary as the hydraulic head would be affected by any changes in the tidal range and the time available for discharge is dependent on the duration of the falling tide (tidal duration asymmetry). Comparing the drainage window duration-elevation curve for various catchments can provide an indication of the relative drainage risk throughout an estuary. Additionally, estimating the drainage window under varying hydrodynamic or catchment conditions can provide insights into how natural and anthropogenic changes may impact the drainage of coastal and estuarine floodplains. This study uses SLR as an example, as it is expected that changing water levels would affect the drainage window throughout the full tidal range, with the extent of these changes reflecting varying hydrodynamic characteristics of the estuary. For instance, where a rise in water level results in dampening of the tidal range (Figure 2(a)), the reduction in the drainage window would be greater at elevations below, and less at elevations above, the mid-tide level. Under either existing or future conditions, dampening of the tidal range would enhance the opportunity for discharge to levels above the mid-tide height compared to tidal amplification (Figure 2(b)), while reducing the drainage window available at lower levels. Dampening of the tidal range is typically experienced where the effects of friction dominate the tidal wave energy or there is an expansion in the area of flow, for example where low-lying land is inundated or channel banks diverge (Khojasteh, Glamore, et al., 2021; Talke & Jay, 2020). Conversely, tides may be amplified by a gradual contraction in the width or depth of an estuary (respectively termed funnelling and shoaling) or by reflection or resonance of the tidal wave (Khojasteh, Glamore, et al., 2021; Talke & Jay, 2020). The net effect on estuarine water levels will depend on the relative impact of each of these influences (Friedrichs, 2010).

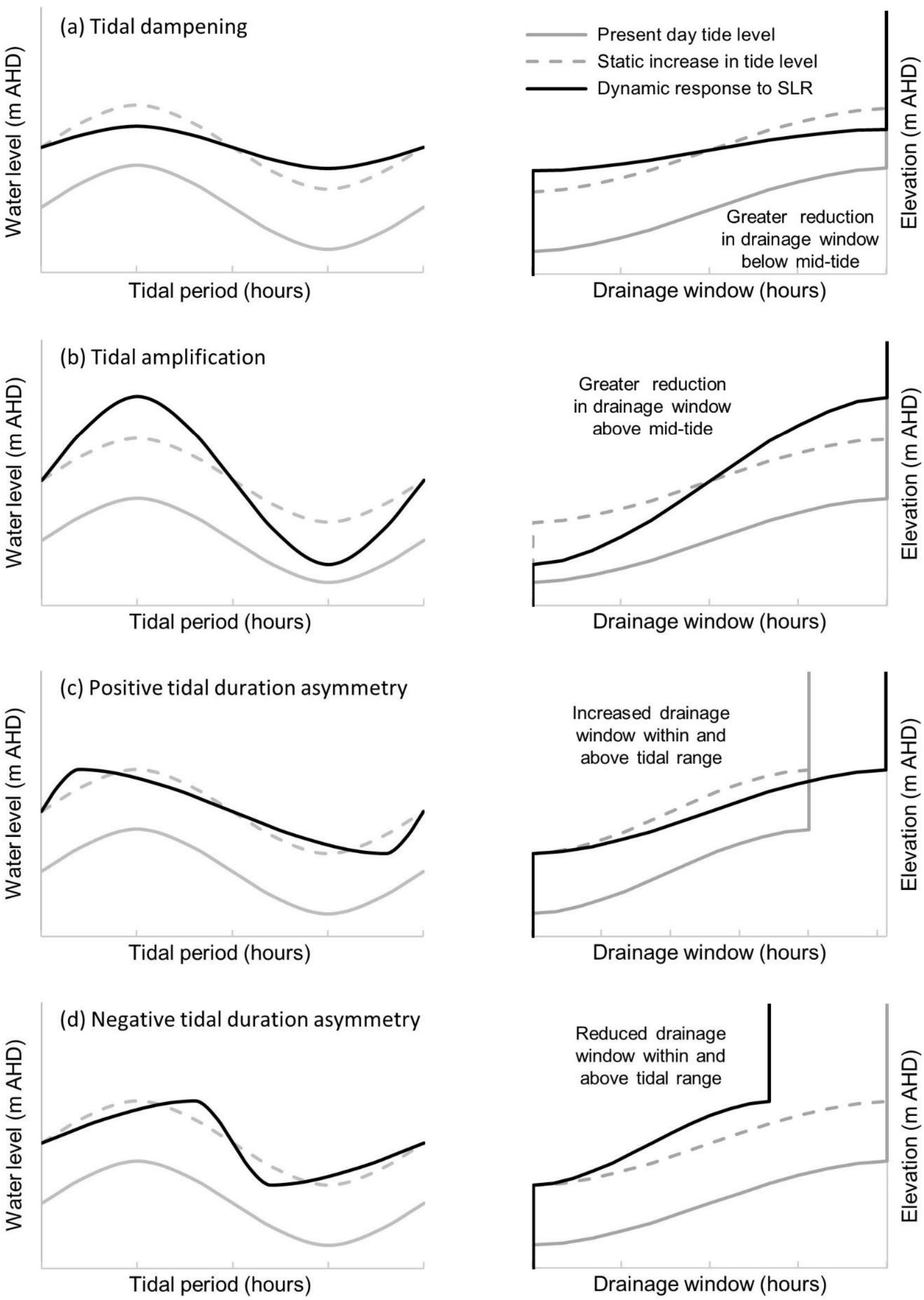

Figure 2 Impacts on a conceptual drainage window (DW) resulting from (a) dampening or (b) amplification of the tidal range and (c) positive or (d) negative tidal duration asymmetry compared to that of a static increase in water levels under SLR. The impacts of changes to the

tidal range vary about the mid-tide (mean water level), with opposite effects at high and low water levels.

Where one-way floodgates have been installed at or below the low tide level, drainage during the rising tide would be precluded during dry weather conditions. A reduction in the duration of the rising tide (positive tidal duration asymmetry as indicated in Figure 2(c)) would therefore increase the drainage window over all water levels compared to areas experiencing shorter falling tides (negative tidal duration asymmetry as indicated in Figure 2(d)). Within estuaries, water level or tidal duration asymmetry is often associated with compound overtides caused by changes in energy associated with friction and channel convergence (L. Guo et al., 2015). Tidal duration asymmetry does not necessarily align with tidal current asymmetry (Gallo & Vinzon, 2005), although many of the forcing mechanisms can be similar as a shorter rising tide may lead to stronger flood currents in the absence of significant fluvial discharges (L. Guo, Wang, Townend, & He, 2019). Positive tidal duration asymmetry (flood dominance) is typically encountered when friction is reduced as the depth of flow increases (Friedrichs & Aubrey, 1994), often where estuaries feature shallow inlet systems or large inter-tidal storage (W. Zhang et al., 2018). It may also result from increasing water levels due to SLR. Conversely, where new or existing inter-tidal or overbank areas are activated by the rising tide, or by SLR for example, increasing friction may reduce the available drainage window by inducing negative tidal duration asymmetry.

To accommodate the dynamic effect of different astronomical and seasonal conditions, a statistical analysis of a representative time series of tidal cycles (*n*) is required to describe the drainage window at any particular location across an estuary. Each of these tidal conditions will provide a different drainage response and identify different vulnerabilities. This study was intended to provide a baseline description of drainage potential throughout each of two estuaries, so the average drainage window available at major drainage outlets (floodgates) was calculated for a mean annual time series of water levels modelled on dry weather conditions:

$$DW_h\,(mean) = \frac{1}{n}\sum_{tidal\ cycle}^{n} \quad t(h) - \ t(LT) \qquad (2)$$

2.2 Study sites

The estuaries of the Hastings and Clarence Rivers were selected to test the drainage window concept across multiple catchments within different estuaries, as these two systems provide insights into how the drainage window will respond to varying tidal range, tidal duration and estuary geometry under different SLR scenarios. The Hastings (Figure 3) and Clarence (Figure 4) Rivers are located in north-east NSW, Australia. Each river has a shallow estuary with a trained entrance that has been stabilised to prevent migration and permit regular exchange of the semi-diurnal tide. The average offshore mean tidal range increases from 1.95m at the Hastings River, north along the coast to 2.04m at the Clarence River (Couriel, Alley, & Modra, 2012). The Clarence River is the largest coastal river in NSW, with the estuarine section reaching 110 km inland and incorporating extensive intertidal areas. These features provide an opportunity to examine the effect of varying tidal characteristics on the drainage window compared to the Hastings River estuary, where the main arm is only 36 km long and the variation in the tidal range is 37% of that experienced in the Clarence River estuary (Couriel et al., 2012.). Characteristics of the studied estuaries are presented in Table 1.

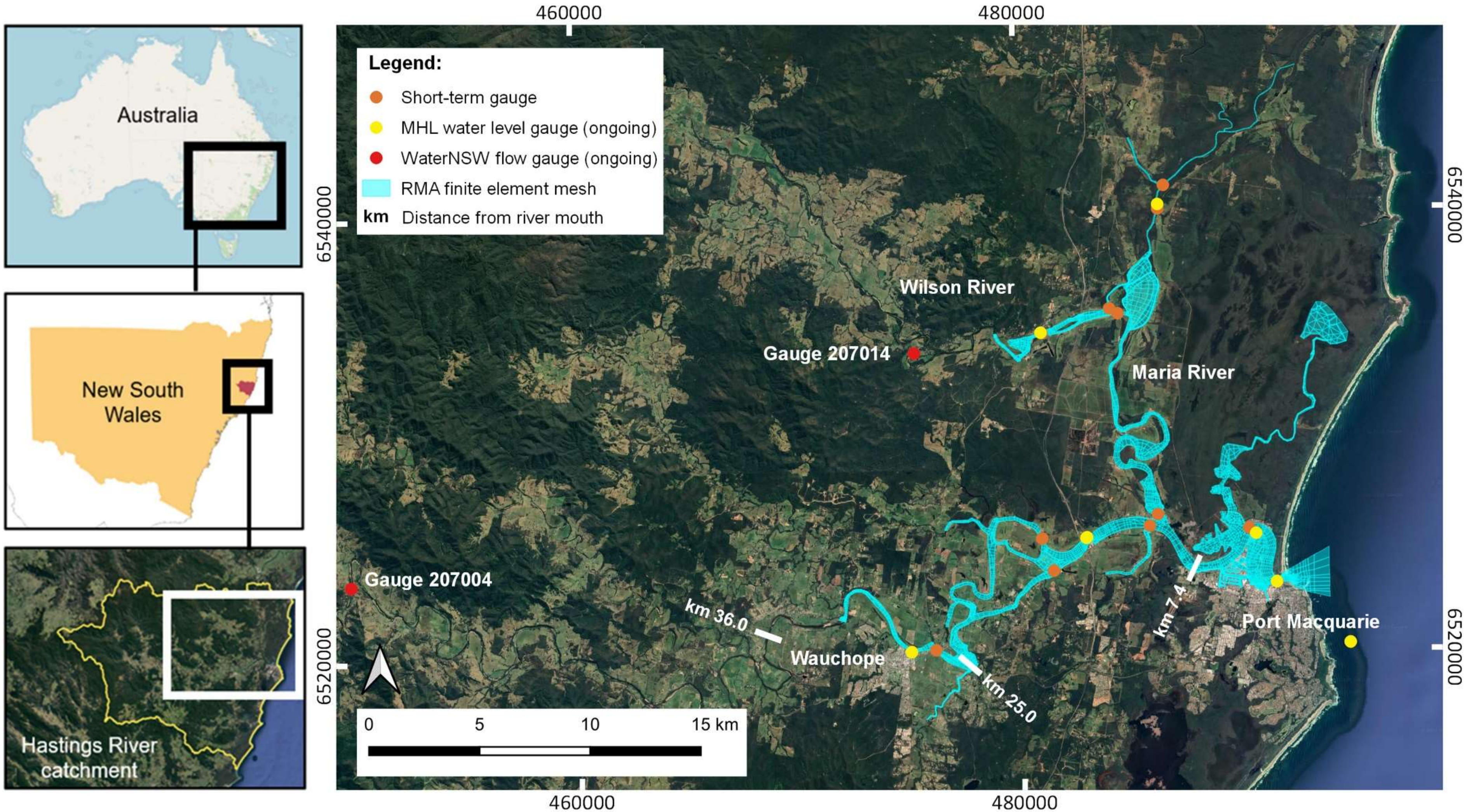

255

256 **Figure 3** Location of study area and extent of RMA-2 hydrodynamic model for the Hastings River

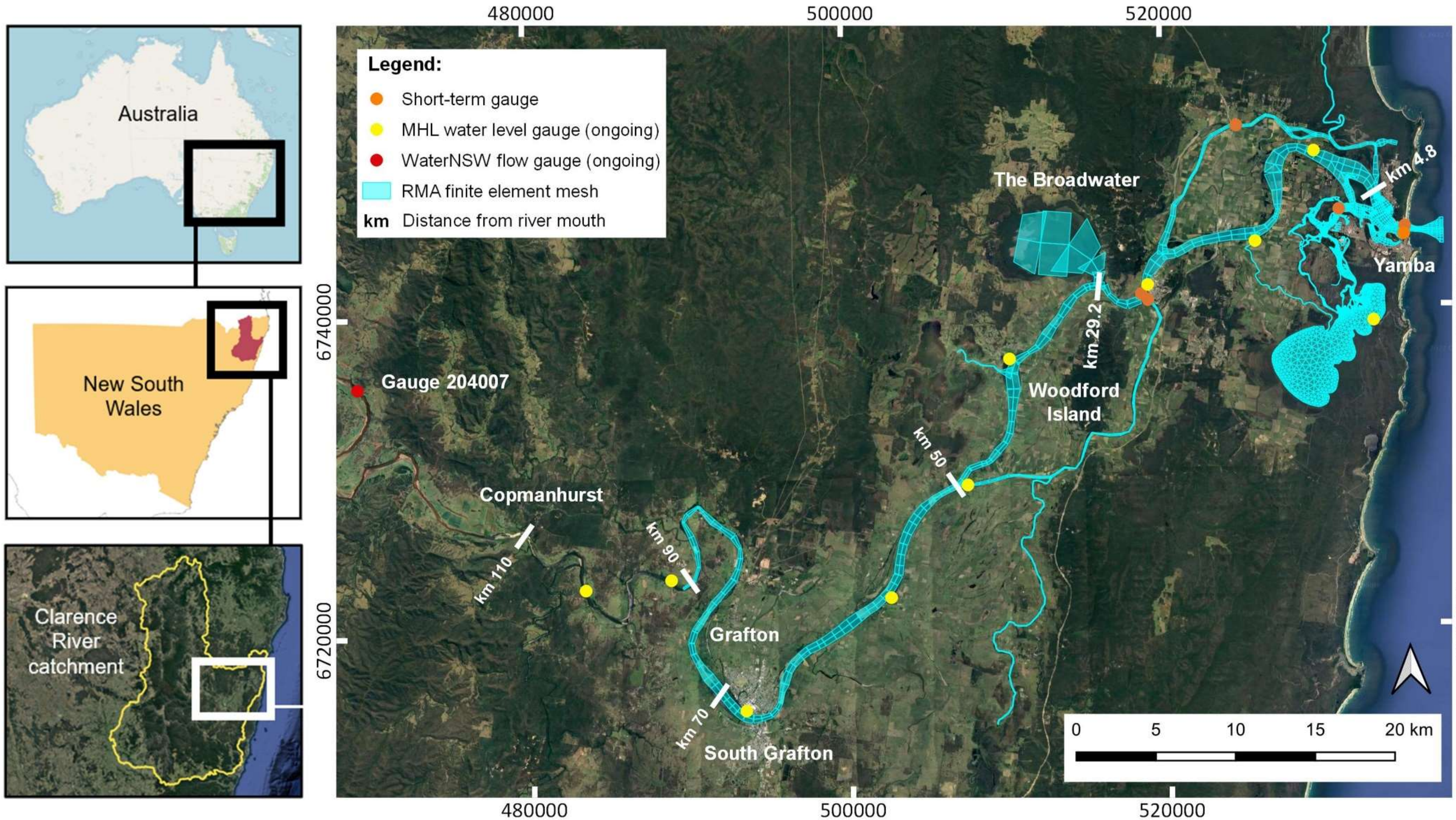

Figure 4 Location of study area and extent of RMA-2 hydrodynamic model for the Clarence River

Table 1 Characteristics of studied estuaries.

Estuary	Catchment area[a] (km^2)	Estuary area[a] (km^2)	Estuary volume[a] (ML)	Estuary length[a] (km)	Average depth[a] (m)	Tidal range[b] (m)
Hastings River	3,659	30	52,690	36[c]	1.9	1.157 – 1.668
(Wauchope to Port Macquarie)		(0.8%)				
Clarence River	22,055	132	283,000	110[d]	2.2	0.477 – 1.822
(Grafton to Yamba)		(0.6%)				

Notes: [a] Environment NSW (2020) [b] Spatial variation in tidal plane range calculated by subtracting the Indian Spring Low Water from the High High Water Solstice Springs (HHWSS – ISLW) (Couriel et al., 2012) [c] Tidal limit surveyed in 1998 (Allsop, 2006) [d] Tide stopped by rocky rapids at Copmanhurst, surveyed 1997 (Allsop, 2006)

2.3 Hydrodynamic modelling and water level data

Detailed hydrodynamic models of the estuarine sections of the Clarence and Hastings Rivers were developed using the RMA-2 suite of models (developed by Resource Modelling Associates) to generate long-term, continuous water level data that can be used to determine the statistical distribution of the drainage window. RMA-2 has been widely used to represent tidal estuaries (Elmoustafa, 2017; Hottinger, 2019; Proudfoot, Valentine, Evans, & King, 2018). The model solves depth-averaged, shallow water wave equations using the Reynolds' form of the Navier-Stokes equation for turbulent flows to calculate water levels and flow velocities at each node of a flexible, two-dimensional mesh (King, 2015).

The model development, calibration, and verification are detailed by (Harrison, 2022a) for the Clarence River and (Harrison, 2022b) for the Hastings River. In summary, the RMA-2 finite element mesh was varied to represent the irregular configuration of each estuary, providing higher resolution at locations with more complex energy transitions such as lagoon entrances, junctions, and bends, as indicated in Figures 3 and 4. The channel cross-sections become more regular in the upper reaches of each estuary, which were modelled using one-dimensional elements. Model bathymetry was obtained from detailed spatial surveys undertaken between 2014 and 2020, with the most recent data given preference. All levels are relative to the Australian Height Datum (AHD), with 0.0 m AHD representative of the average oceanic mean sea level around the Australian coast.

Upstream and downstream boundary conditions were defined by gauged catchment inflows and oceanic tide levels respectively. Long-term water level and short-term flow gauges throughout each catchment were also used for model calibration, which was undertaken by adjusting the Manning's 'n' roughness coefficients, with adopted values varying from 0.020 to 0.023 in the main channels, up to 0.045 in tributaries. The models' ability to represent a range of tidal conditions throughout each estuary was then verified by simulating both 'wet' (2013) and 'dry' (2019) rainfall years, the selection of which was based on historic rainfall records. The water level and flow gauge locations used for boundary conditions, calibration, and verification of the model are indicated in Figures 3 and 4, with the historical variability in the recorded flow data at the upstream boundaries presented in the Supporting Information and summarised in Table 2. This data indicates median catchment inflows for the representative 'dry' year of 2019 were no more than 20% of the long-term median flow rates (January 2000 to December 2019). The total annual rainfall for 2019 was 481mm in the Hastings catchment (represented by gauge 207004, Figure 3) and 398mm in the Clarence catchment (gauge 204007, Figure 4), compared to long-term averages of 1,124mm and 1,293mm respectively (January 2000 to December 2019). The boundary conditions defined by the representative 'dry' year were adopted for the drainage window analysis to mitigate the impact of catchment hydrology and to isolate, as far as possible, the effect of SLR on the drainage window during non-flood periods. Under these conditions, the mean annual low tide (modelled) lies within the range of operation (invert level to obvert level) of the floodgates servicing the major drainage systems. Full details of the floodgate levels, culvert dimensions and low tide ranges for each of the major drainage systems within the studied catchments are provided in the Supporting Information.

Table 2: Historic river flow data for the Clarence and Hastings Rivers.

	Exceedance				
River flow (ML/d)[a]	**0%**	**25%**	**50%**	**75%**	**100%**
Clarence River (gauge 204007)					
2000-2019	10	775	1,782	4,513	1,132,954
2019 (dry year)	10	198	372	657	2005
Hastings River (gauge 207004)					
2000-2019	0	163	385	971	239,828
2019 (dry year)	0	17	51	94	349
Wilson River (gauge 207014)[b]					
2000-2019	0	23	81	241	98,041
2019 (dry year)	0	0	3	11	73

[a] Sourced from WaterNSW for 1 January 2000 to 31 December 2019. Refer to Supporting Information.
[b] Wilson River is a tributary of the Hastings River, refer to Figure 3.

Varying downstream boundary conditions were applied to reflect the present-day, near- and far-future SLR scenarios (refer to Section 2.4). No changes were made to the catchment inflows. Water levels were extracted at hourly timesteps at the main drainage discharge locations for each catchment throughout both estuaries (located between 5 km and 29 km along the Hastings River, and between 5 km and 70 km along the Clarence River, with major floodgate locations in the Supporting Information) and used to determine the drainage window (the difference in time between each nominated level and the subsequent low tide) at 0.1 m increments in elevation.

The results were firstly assessed on a catchment basis to identify local drainage conditions and how they may be impacted by SLR. As chronic conditions are established by persistent rather than intermittent exposure, an analysis of the mean annual drainage window was undertaken to identify the underlying drainage conditions at each discharge location. Thus the maximum drainage window represents the maximum (mean) annual duration of the falling tide, with the minimum corresponding water level identified as the critical elevation below which the catchment would experience a persistent reduction in the available drainage window. Similarly, the zero value for the mean annual drainage window is a conservative representation of the lowest annual low tide, as the mean annual low tide (to which the catchment can consistently drain) would normally be higher. Progressive longitudinal changes in the mean annual drainage window at key drainage outlets along each estuary were then compared to changes in the tide duration asymmetry and the tidal range to identify the extent to which these factors may contribute to drainage risk.

For the purposes of this study, the calculation of tidal duration asymmetry and tidal range has been based on the same modelled water levels used to determine the drainage windows. Tidal duration asymmetry was calculated as the duration of the falling tide compared to the total tidal cycle averaged over the annual time series. This is an annual mean interpretation of tidal skewness as presented by (Nidzieko, 2010), whereby a positive tidal asymmetry (positive skewness) is indicative of a longer falling tide (Song, Wang, Kiss, & Bao, 2011; W. Zhang et al., 2018). The tidal range was represented by the difference between the maximum and minimum water levels generated by the model over the annual time series.

2.4 Sea level rise scenarios

The impact of SLR on the estuarine water levels was modelled by adjusting the downstream tidal boundary condition to reflect near-future (NF) and far-future (FF) sea levels. Locally adopted SLR benchmarks of +0.4 m by 2050 and +0.9 m by 2100, relative to the mean sea level (MSL) of 1996, were applied (Glamore, 2016). These values represent the median for the representative concentration pathway (RCP) 8.5 scenario (Pachauri et al., 2014) and are the most up to date values specific to the NSW coastline consistent with the Shared Socioeconomic Pathway, SSP5 (Masson-Delmotte et al., 2021). To account for SLR that has occurred between 1996 and 2020, downstream tidal water levels were increased by +4.5 mm/year, as per White et al. (2014), so that all water levels applied in the hydrodynamic models are relative to 2020, nominally the present-day (. Values for mean sea level applied to the downstream boundaries of each hydrodynamic model for the near- and far-future cases, relative to the present, are presented in Table 3.

Table 3 Oceanic boundary SLR predictions for NSW, representing near-future (NF) and far-future (FF) scenarios adjusted to present-day (PD).

	NF (2050)	**FF (2100)**
RCP 8.5 - median SLR relative to MSL 1996	+ 0.27 m	+ 0.78 m
SLR from 1996 to 2020 @ 4.5 mm/year	+ 0.11 m	+ 0.11 m
Adopted SLR relative to PD (2020)	+ 0.16 m	+ 0.67 m

2.5 Topographic data

By adopting the same vertical datum for both topographic and water levels, the drainage window analysis can be used to provide an indication of the vulnerability of floodplain catchments to reduced drainage. To this end, one-metre resolution digital elevation models (DEMs) were sourced from the National Elevation Data Framework spatial dataset (Geoscience Australia, 2020) to represent the catchment topography for each estuary. The data is reported to have an accuracy of 0.3 m in the vertical direction and 0.8 m horizontal.

The QGIS geographic information system was used to process the DEMs. Discrete catchment areas for each of the major drainage systems were defined based on the floodplain topography, including consideration of the connectivity of watercourses, drains and major floodplain infrastructure.

The hypsometric curve function in QGIS was used to plot the cumulative area against 0.1 m increments in elevation for each catchment to enable a direct comparison between the local topography and critical drainage levels. This 0.1m increment is representative of the uncertainty in the calibration of water levels in the hydrodynamic models and must be considered in addition to the accuracy of the DEM. The topographic extent to which changes in the drainage window may impact the floodplain catchments, as mapped in Section 3, should therefore only be considered indicative.

QGIS was also used to map the topographic levels corresponding to the water levels that represent the zero and maximum mean drainage window durations, as well as that representing a 50% reduction in the maximum. During dry conditions, flows within the catchment drainage channels would be isolated from the tidal perturbations of the main estuary by the floodgates and low flow velocities would not incur significant head losses, so while the assumption of a static transfer of water levels from the estuary to the drainage catchment is a simplified approach, it is considered suitable to provide an indication of the extent of the area that would be affected by reduced drainage within each catchment.

3 Results

3.1 Drainage window analysis of exemplar catchment

An analysis of the drainage window under present-day, near- and far-future scenarios is illustrated in Figure 5 for the western side of Woodford Island. Woodford Island is situated between 34 km and 55 km upstream of the mouth of the Clarence River (Figure 4), east of a large intertidal lagoon known as The Broadwater. Natural watercourses have been adopted, modified, and supplemented by constructed channels to improve floodplain drainage (Figure 5(a)) and enable discharge to the present-day lowest tide at -0.3 m AHD (mean zero drainage window for simulated dry year). Floodgates and levees around the island perimeter (Figure 5(a, b)) would protect against the highest annual water levels predicted under both present-day (maximum predicted water level of 0.84 m AHD) and far-future (maximum 1.61 m AHD) dry year scenarios. Currently, less than 5 km^2 of the 37 km^2 catchment would be unable to drain over the maximum drainage window of 6.5 hours (Figure 5(c, d)). The capacity of the catchment drainage channels is indicated by the level of the drainage window at the top of bank in Figure 5(e-f). In the far-future scenario, the low tide (zero drainage window) would have at a minimum level of +0.3 m AHD. This would render 23% of the existing drainage channels ineffective, with a standing water level at the top of bank (100% reduction in drainage window). The drainage window for 59% of the channels (all drainage infrastructure below 0.7 m AHD) would be reduced between 50% and 100% (Figure 5(g)). Thus, despite an apparently strong degree of protection from inundation by high water levels, the area affected by a reduced drainage window has the potential to cause extensive waterlogging throughout the catchment in the far-future.

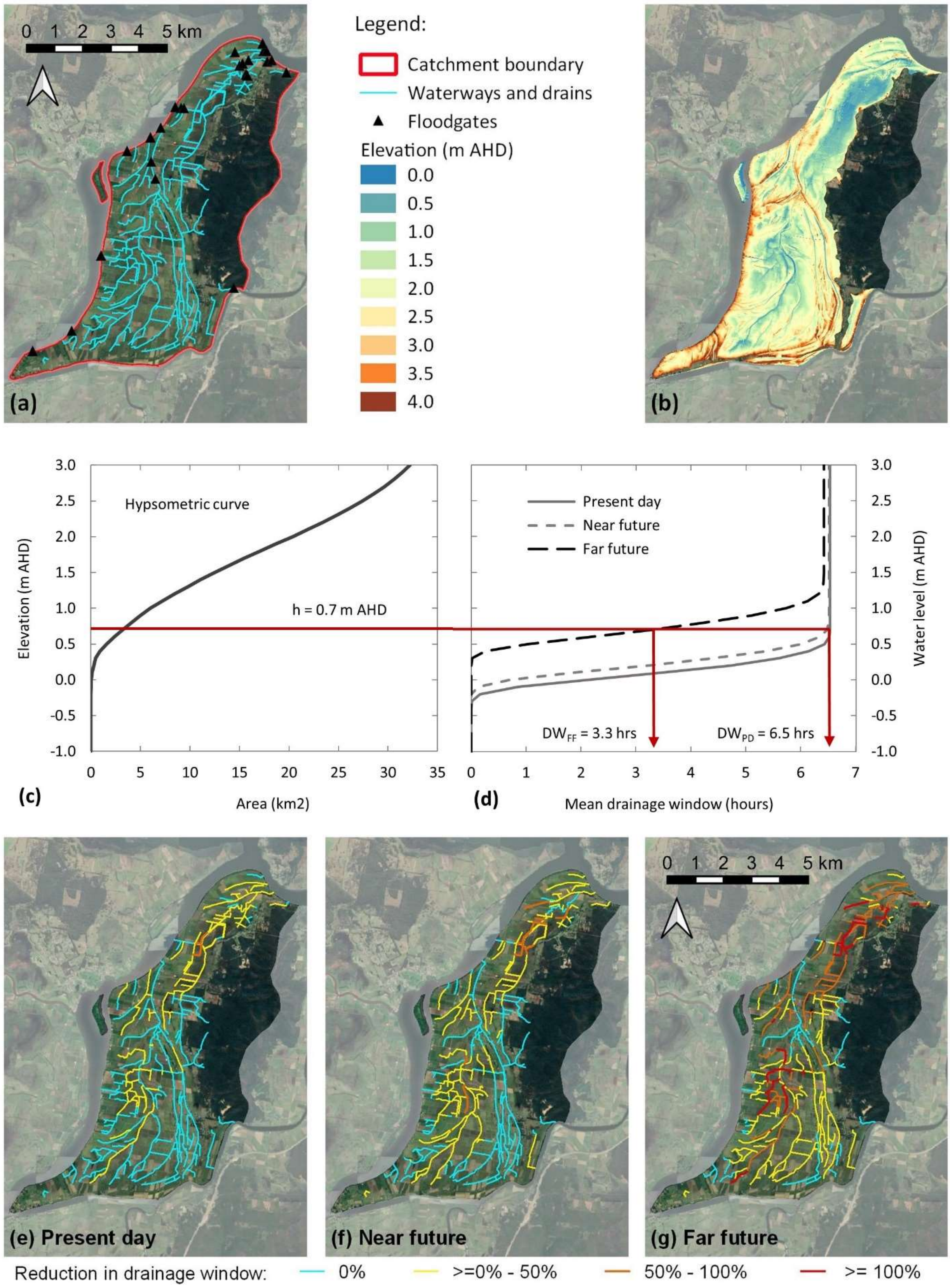

Figure 5 Drainage window (DW) analysis for western Woodford Island. The catchment has a network of natural and constructed drainage channels (a), with catchment topography (b) indicating the perimeter of the island is protected from high water levels by natural and constructed levees. As indicated on the hypsometric curve (c), over 1,400 ha would be

affected by a reduced drainage window, with a 3.2 hour reduction in the mean drainage window (d) at 0.7 m elevation. The extent of the catchment affected by a limited drainage window is presented for (e) present-day, (f) near- and (g) far-future scenarios.

The floodplain extent that would be directly affected by a reduced drainage window is presented in Table 4 and shown in Figure 6 for the Hastings River estuary and in Figure 7 for the Clarence River estuaries under present day, near- and far -future scenarios. Comparing these results with Figure 5 indicates that there would be extensive waterlogging due to reduced drainage throughout each estuary. Currently, as indicated in Table 4, the Hastings River, and all but 2 ha of the Clarence River's estuarine floodplains, discharge freely to the low tide at some stage of the tidal range. However, under the far-future scenario, SLR would increase the area of impeded drainage by over 70% in both estuaries. Unless a pumped discharge scheme was implemented, 2,499 ha of the Clarence River estuarine floodplain would be unable to drain, with low-lying backswamp and lagoon foreshore areas identified as being particularly susceptible to reduced drainage.

Table 4: Floodplain area directly impacted by limited drainage window under different SLR scenarios.

		Area (ha) with drainage window limited[a] by:		
Estuary	**Scenario**	**≥ 100%** (no drainage window)	**50%**	**0%**
Clarence	Present-day	2	896	20,100
	Near-future	6	2,948	23,635
	Far-future	2,499	15,202	34,474
Hastings	Present-day	0	132	8,480
	Near-future	0	124	10,898
	Far-future	124	3,371	15,913

[a] when compared to drainage window achieved over full duration of the falling tide.

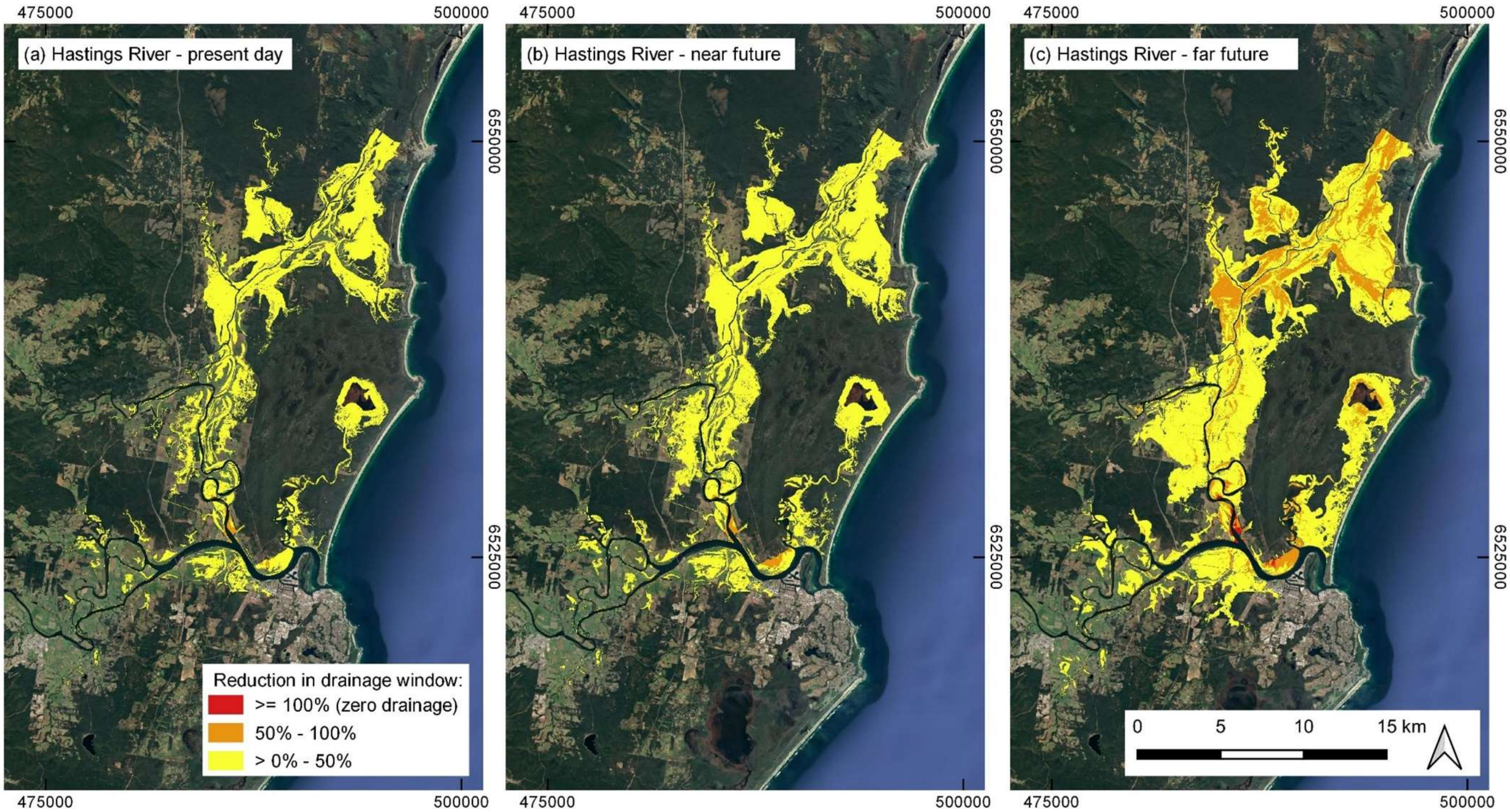

Figure 6 Extent of estuarine floodplain impacted by limited drainage in the Hastings River for (a) present-day, (b) near- and (c) far-future scenarios.

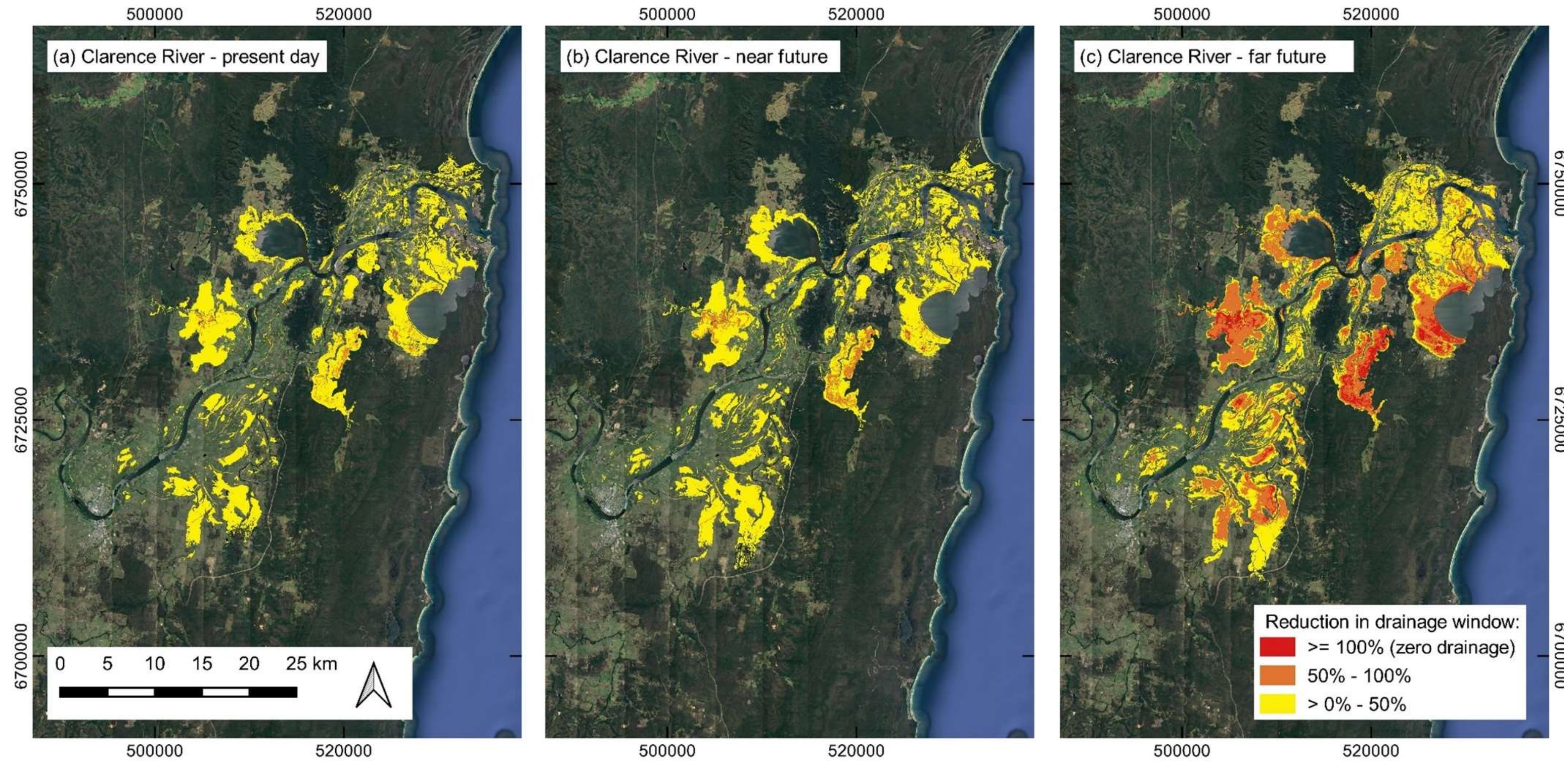

Figure 7 Extent of estuarine floodplain impacted by limited drainage in the Clarence River for (d) present-day, (e) near- and (f) far-future scenarios.

3.2 Variation in the drainage response along an estuary and under SLR

Under both present day (Figure 8(a, b)) and far-future (Figure 8(c, d)) conditions, the drainage window varies in response to changes in the tidal range and the tidal duration asymmetry as the tide propagates along the Clarence and Hastings Rivers. In the lower reaches of both estuaries, a deltaic network of anabranches and shoals create shallow water conditions that enhance energy dissipation, contributing to tidal dampening and an increase in the duration of the falling tide. The effects of large flow bifurcations are noticeable at the Maria River (km 9.3) in the Hastings River estuary and at The Broadwater (km 29.2) in the Clarence River estuary. At these junctions, increasing hydraulic losses at higher water levels slow the propagation of the rising tide and reduce the duration of the falling tide, resulting in a corresponding reduction in the available drainage window. This effect is particularly pronounced around The Broadwater, where low-lying wetlands provide extensive intertidal storage capacity. Continuing upstream, convergence effects tend to amplify the tidal range in the upper reaches of each estuary, where the tidal wave is confined within the main channel and, as shown in Figure 8(e, f), both estuaries exhibit a tendency for a progressive extension in the duration of the falling tide.

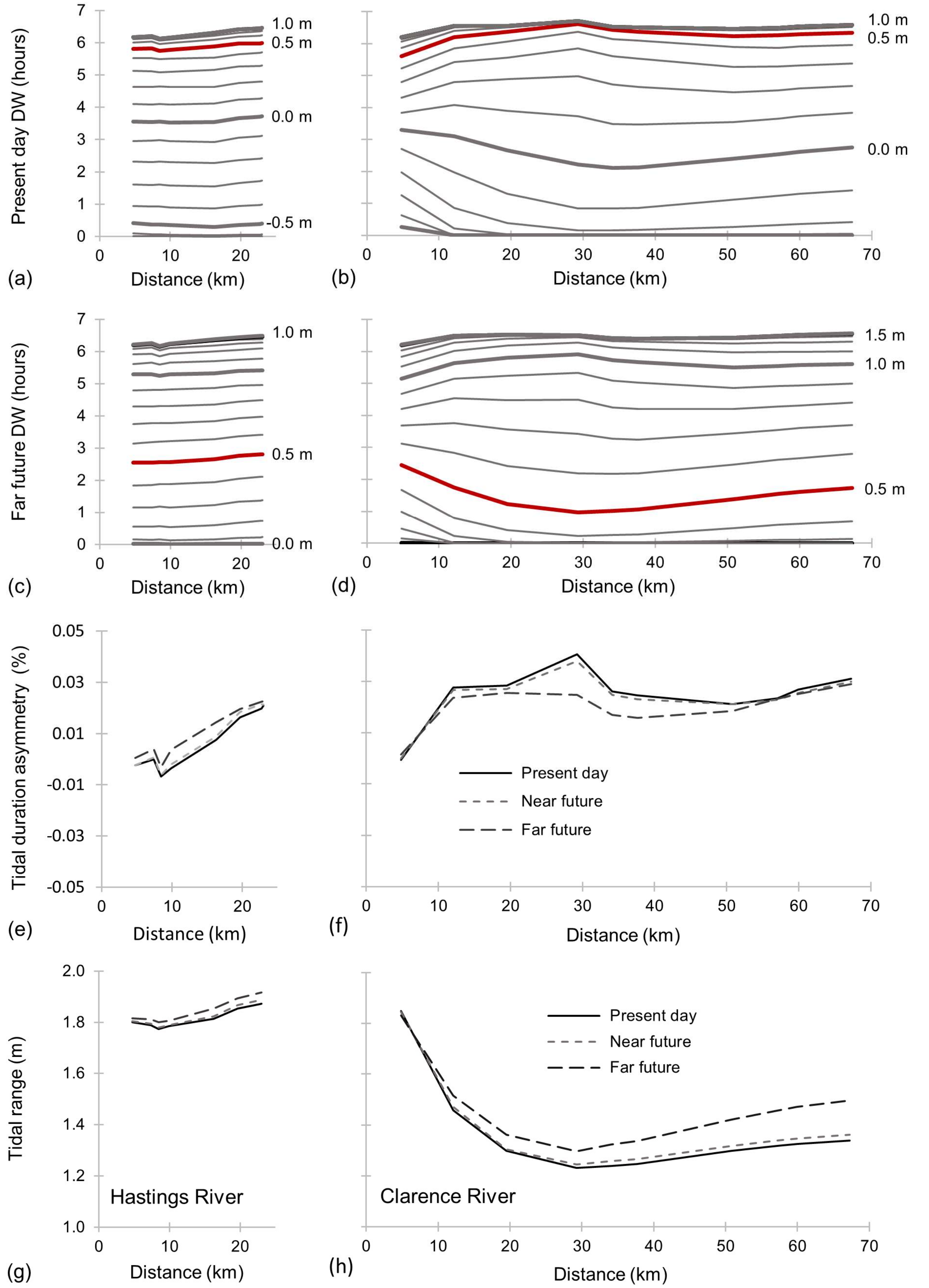

Figure 8 Longitudinal changes in the mean annual drainage window, tidal duration asymmetry and tidal range with distance from the river mouth calculated using water levels modelled for the representative dry year (2019). Variations in the drainage window (DW) under present day (a, b) and far-future (c, d) scenarios at 0.1 m increments for the Hastings (left) and

Clarence (right) River estuaries. The red line highlights the future reduction in the drainage window at a level of 0.5 m AHD. The variations in the drainage window reflect changes in the tidal duration asymmetry (e, f) and changes in the tidal range (g, h) along the Hastings and Clarence Rivers from the estuary mouth (km 0). Tidal range was measured as the difference between the annual maximum and minimum water levels during the modelled dry year. Changes in the drainage window are particularly pronounced at changes in hydrodynamic conditions such as the Maria River junction (Hastings River km 9.3) and The Broadwater (Clarence River km 29.2).

In the main arm of the Hastings River estuary, changes to the tidal characteristics are presently limited, with the effects of channel convergence approximately balanced by frictional losses. For any nominated water level, the drainage window does not vary by more than 0.5 hours throughout the estuary. Similarly, there is minimal variation in the tidal range, falling tide duration or drainage window under the future SLR scenarios (Figure 8(c)). The results are similar to those that would be achieved by the static addition of +0.67 m SLR to present day water levels, although in the far-future scenario, a lengthening falling tide duration (Figure 8(e)) coupled with minor tidal range amplification (Figure 8(g)), would slightly reduce the influence of SLR on the drainage window. Throughout the estuary, gravity discharge would currently be available to a minimum level of -0.6 m AHD (Figure 8(a)), increasing to 0.0 m AHD in the far-future (Figure 8(c)).

Both the tidal duration asymmetry (Figure 8(f)) and tidal range (Figure 8(h)) are more varied along the length of the Clarence River estuary. This can be largely attributed to energy losses associated with a complex network of anabranches, channels and shoals, and the diversion of flows into extensive shallow lagoon areas. In contrast to the relatively homogeneity of the response in the Hastings River (Figure 9(a)), comparing the drainage window (Figure 9(b)) of a catchment near the mouth of the Clarence River (at km 4.8, as indicated in Figure 4, this is most representative of undistorted tidal conditions) with one near the point of maximum tidal distortion (km 29.2) reveals the longer falling tide would increase the upstream drainage window by up to 0.5 hours in the present-day and 0.3 hours in the far-future scenario. Under current conditions, this would be augmented by the effects of tidal dampening above the mid tide level of 0.2 m AHD. Below the mid tide level, the drainage window would be reduced by up to 1.9 hours at a level of -0.1 m AHD. Higher water levels under future SLR scenarios would reduce the degree of tidal dampening and the maximum reduction in the drainage window would be limited to 1.5 hours at a level of 0.5 m AHD. However, the most substantial change in both estuaries is the reduction in the drainage window resulting from an elevated tidal range under SLR.

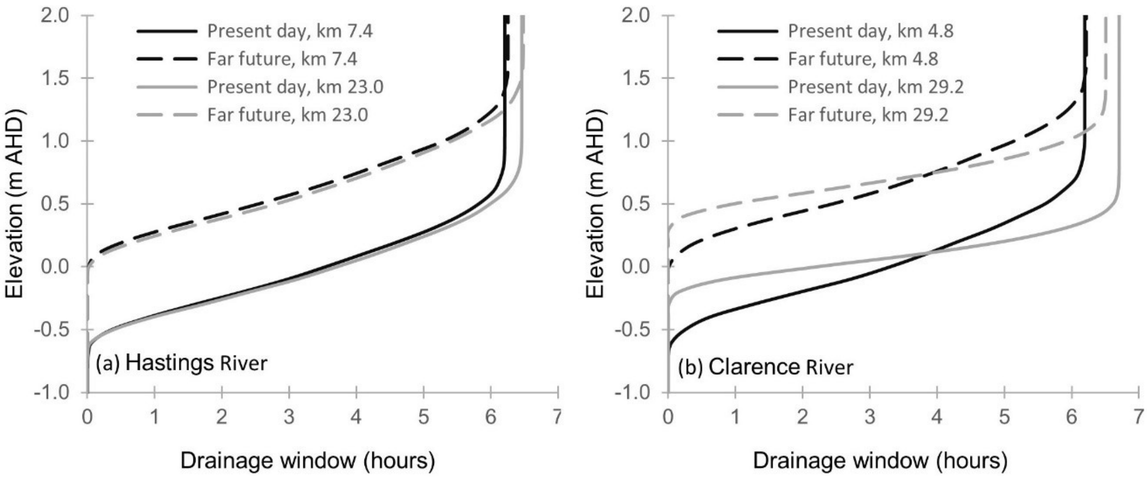

Figure 9 Changes in the drainage window (DW) from the mouth of the estuary upstream to the location displaying the greatest change in the drainage window for the Hastings (a) and Clarence (b) Rivers under present-day and far-future scenarios. The changes in the Hastings River estuary (a) show little variation between sites. In the Clarence River estuary, tidal dampening at km 29.2 reduces the drainage window below the mid tide level. The increase in the drainage window above the tidal range reflects the longer duration of the falling tide in the future. The impacts of SLR dominate the change in the drainage window under the far-future scenario.

4 Discussion

To date, studies regarding the potential impacts of SLR on low-lying floodplains have primarily focused on the increased risk of intermittent flood and storm inundation associated with altered high tide levels. In contrast, the reduction in the drainage window predicted in this study highlights the chronic pressures likely to affect floodplain drainage systems. The actual impact realised by a reduced drainage window will depend on the local drainage efficiency, the volume of storage available within the catchment and how much water needs to be discharged, whether this is from excess irrigation, wastewater, intercepted groundwater, or rainfall runoff. While this study has focussed on chronic drainage conditions by investigating the impact of SLR during a period of relatively dry weather, reduced drainage during wet weather and flood conditions may have an even greater impact on coastal land management. The effects of river discharge on tidal propagation are highly dynamic (Cai et al., 2019; L. Guo et al., 2019). Increasing river discharge can not only raise water levels, but also increase tidal wave deformations (Godin, 1985; L. Guo et al., 2015), putting added pressure on the drainage window. Typically, higher river flow will dampen the tidal range (Díez-Minguito et al., 2012; L. Guo et al., 2015) although at various flow rates this effect may simultaneously amplify it in lower reaches of the river (Dykstra, Dzwonkowski, & Torres, 2022). Flood studies typically isolate extreme events, limiting their assessments to a number of days, or even hours, before and after the flood peak (Helaire, Talke, Jay, & Chang, 2020; Hsiao et al., 2021; P. M. Orton et al., 2020). However, where the flood recession is impacted by tidal conditions, a reduced drainage window is likely to substantially prolong the recession period. The results of this study highlight the need for further investigation into the potential for the extended flood recession period from a rainfall event to coincide with the onset of a subsequent event(s), leading to extensive prolonged inundation and profound implications for existing land uses.

It has been suggested that the flood hazard characteristics of many estuarine systems could be aggregated into coastal, transitional, and fluvial regions, with different sensitivities to changing climate conditions in each (Helaire et al., 2020). Similarly, many estuaries are likely to exhibit zones of varying drainage hazard, as exemplified by the results for the Clarence River herein. High risk drainage areas (those with short drainage windows) are associated with tidal dampening or positive water level asymmetry. Tidal dampening is commonly associated with longer estuaries, estuaries which are prismatic or weakly converging, or those with restricted entrances (Khojasteh, Chen, et al., 2021). Areas with extensive intertidal flats are also susceptible to tidal dampening (Du et al., 2018; Lee, Li, & Zhang, 2017). In these areas, typified by shallow coastal lagoons and backswamps, the reduction in the drainage window due to tidal dampening may be exacerbated by a reduction in the duration of the falling tide. Variations in the drainage window throughout the Clarence Estuary are more strongly affected by the impact of changes to the tidal range than tidal duration asymmetry, which is reflected in the fact that the principal astronomic constituents (M_2, S_2, K_1 and O_1) account for over 95% of the annual average tidal range measured throughout the estuary (Couriel et al., 2012). Conversely, the impact of tidal duration asymmetry is more substantial in the Hastings Estuary, where the overtides contribute to over 10% of the total tidal amplitude (Couriel et al., 2012). These impacts remain relatively minor as the Hastings Estuary was found to display a comparatively static response to the tide. This comparison, however, highlights significant potential to identify areas that are particularly susceptible to a reduced drainage window as a result of tidal duration asymmetry by examining the generation of overtides and compound tides.

The modelling undertaken for this study does not address uncertainties around anthropogenic, geomorphic, or vegetative adaptations to SLR. As flood and drainage conditions worsen, it is highly likely that there will be trade-offs between protecting reclaimed lands and retreating from them that will further impact the hydrodynamic response of the estuary. Additionally, a linear increase in oceanic sea level at the downstream boundary of the models has been assumed, with present-day catchment inflows used at the upstream boundary for all model scenarios. All of these variables are likely to result in complex feedback loops with dynamic impacts on the tidal range. However, despite these limitations, the modelling highlights that SLR is likely to result in prolonged periods of reduced drainage that are likely to lead to higher groundwater levels, soil waterlogging, and the permanent inundation of low-lying areas.

Varying responses to changes in water levels may redefine which areas within the estuary are more adversely affected by limited drainage conditions. For example, in many highly developed areas, such as the San Francisco Bay (Holleman & Stacey, 2014) and the Chesapeake and Delaware Bays (Lee et al., 2017), shoreline protection works have channelised tidal flows, leading to an amplification of the tidal range. Holleman and Stacey (2014) note that concerns have been raised that further reinforcement of the shoreline for flood protection from rising sea levels may increase tidal amplification, with higher peak water levels increasing the associated flood risk to adjacent areas, as has occurred following tidal-flat reclamation along the Shanghai coast of China (M. Zhang et al., 2021). Conversely, numerous studies have highlighted the role of energy attenuation for storm protection, examining opportunities to reduce channel depths and increase shallow wetland areas in Jamaica Bay, New York (Philip M. Orton et al., 2015), or install artificial sandbanks in the Elbe River Estuary (Ohle, Schuster, Kappenberg, Sothmann, & Rudolph, 2017; von Storch, Gönnert, & Meine, 2008) for example. Dampening of the tidal range by facilitating the inundation of low-lying areas has been postulated as an alternative mitigation strategy for future high tide inundation in the Chesapeake and Delaware Bays (Lee et al., 2017) and the use of hybrid flood defence systems incorporating restored tidal marshes is gaining traction (Smolders et al., 2020; Stark, Plancke, Ides, Meire, & Temmerman, 2016). The results presented in this study indicate that tidal attenuation strategies such as these may impede drainage and increase chronic inundation and waterlogging from rising sea levels, s highlighting that consideration of the drainage window may help to provide a holistic assessment of the impacts of changes to water levels through the whole tidal range. These changes are not limited to SLR and include natural and anthropogenic activities such as changes to river flow (Jalón-Rojas, Sottolichio, Hanquiez, Fort, & Schmidt, 2018), sedimentation (Talke & Jay, 2020), dredging (Chant, Sommerfield, & Talke, 2018), channel realignment or armouring (W. Guo, Wang, Ding, Ge, & Song, 2018) as well as land reclamation or wetland restoration (Holleman & Stacey, 2014).

As drainage decreases, numerous floodplain catchments will be faced with economic pressures to protect or preserve existing land use. Historically, the response to these pressures has involved the construction of hard engineering structures such as levees, dykes, seawalls, pumps, and diversion channels to defend vulnerable areas from flooding and/or promote drainage (Day & Templet, 1989). However, the construction, operation, and maintenance of this infrastructure is only viable if it is offset by societal and/or economic returns, such as in the Netherlands (Xu & Blussé, 2019). Consequently, pumped systems are more typically implemented where periodic usage can augment gravity discharge, for example in parts of Australia (Yang, 2008), the USA (Lang, Oladeji, Josan, & Daroub, 2010) and Asia (Marfai & King, 2008). The future expansion of pumped discharge systems would, however, only be economically justifiable where there are adequate commercial returns and may be complicated by environmental issues such as land subsidence (Nicholls, 2015; Talke & Jay, 2020) or acid sulphate soils (Dawson, Kechavarzi, Leeds-Harrison, & Burton, 2010).

Where gravity systems remain the preferred option for drainage management, additional attenuating storage may be required to offset the reduction in drainage capacity. The relationship between the local topography and drainage window for a given catchment can be used to identify areas with sufficient capacity within the existing landscape to provide effective attenuation. Examining variations in the drainage window throughout an estuary and comparing it to catchment topography provides a means of identifying floodplain areas at risk from reduced drainage. As such, the drainage window analysis may complement topographic studies when considering future land use and management options and is particularly beneficial in examining future SLR scenarios. Comparing the hypsometric curve to the anticipated change in water levels resulting from SLR may indicate if (and when) a catchment is likely to experience a rapid increase in vulnerability to inundation (Kane, Fletcher, Frazer, & Barbee, 2015). Extending this analysis to encompass the change in drainage window, as indicated in Figure 5 (c) and (d), would also indicate the susceptibility of a local catchment to drainage risks. In high-risk drainage areas, there may be substantial merit in considering alternative nature-based solutions, including wetland restoration projects which have considerable co-benefits, including improved water quality and ecological values as well as significant potential for carbon sequestration (Gulliver et al., 2020; Raw, Adams, Bornman, Riddin, & Vanderklift, 2021; Sheehan, Sherwood, Moyer, Radabaugh, & Simpson, 2019). In some circumstances, the removal of tidal barriers to low-lying estuarine floodplains may be used as a sacrificial measure to increase flood protection elsewhere in the estuary while creating highly valued coastal and estuarine ecosystems using nature-based solutions to accommodate SLR. This prospect is particularly relevant with the emergence of a global blue carbon market that may incentivise tidal inundation of poorly drained land over other low return agricultural production measures.

5 Conclusion

This study has introduced a 'drainage window' concept to quantify and compare the time available for the effective drainage of estuarine catchments under present-day and future SLR conditions. As a proof of concept, hydrodynamic models of the Hastings and Clarence Rivers' estuaries in Australia were used to simulate tidal responses to varying oceanic water levels under current and future SLR scenarios. Modelling results indicate that the drainage window responds dynamically to changes in tidal characteristics as the tide propagates within an estuary. Tidal dampening and flood dominant tidal asymmetry were highlighted as key contributors to a reduced drainage window. Understanding the interactions between tidal range and tidal asymmetry within an estuary may help quantify potential reductions in the drainage window. This may be particularly important in long prismatic or weakly converging estuaries as they may become increasingly vulnerable to reduced drainage following SLR (Khojasteh, Chen, et al., 2021).

While previous studies have examined the impact of SLR on acute flooding events associated with higher high tides (Ben S. Hague & Taylor, 2021; Hino, Belanger, Field, Davies, & Mach, 2019; Moftakhari, AghaKouchak, Sanders, Allaire, & Matthew, 2018), this research highlights chronic impacts that occur across the full tidal range. In direct contrast to flooding risks, which will be exacerbated by increased tidal amplification, reduced drainage capacity is likely to be more pronounced in areas subject to increased tidal dampening. A thorough assessment of the risks posed by SLR at all water levels is therefore required as the reduction in the drainage window could result in changes to land use and broader management policy. This may provide opportunities for adaptation using nature-based solutions given that shallow coastal lagoon and backswamp areas are particularly susceptible to reduced drainage.

Acknowledgements

This paper has been extended and improved with thanks to considered and generous input from Steven Dykstra, two anonymous reviewers and the editorial staff at AGU publishing. The development of the drainage window concept has been aided by discussions with many staff and students at the UNSW Water Research Laboratory, with particular credit to Grantley Smith, Alice Harrison, Jamie Ruprecht, Priom Rahman and Toby Tucker. The authors would also like to extend our gratitude to Priom Rahman for generating the water level data and to Anna Blacka from UNSW Sydney for her assistance with the preparation of figures. Katrina Waddington is supported by an Australian Government Research Training Program Scholarshiop. Danial Khojasteh is supported by a UNSW Scientia PhD Scholarship.

Data availability statement

Hourly water level data generated by the RMA-2 model and used in the drainage window analysis for the Hastings and Clarence Rivers is available from Researchgate at https://doi.org/10.13140/RG.2.2.28047.87208 (Waddington, 2022). Rainfall, water flow and water level data were downloaded from the WaterNSW Water Information Hub Real-time water data (waternsw.com.au), with the data used in this study, as presented in the Supporting Information, sourced for Station 207004 from https://realtimedata.waternsw.com.au/?ppbm=207004&rs&1&rscf_org, for Station 204007 from https://realtimedata.waternsw.com.au/?ppbm=204007&rs&1&rscf_org, and for Station 207014 from https://realtimedata.waternsw.com.au/?ppbm=207014&rs&1&rscf_org. QGIS software can be freely downloaded from Discover QGIS. Digital elevation data was obtained from the National Elevation Data Framework spatial dataset Elvis (fsdf.org.au) managed by Geoscience Australia Digital Elevation Data | Geoscience Australia (ga.gov.au).

Declaration

The authors declare that they have no known competing financial interests or personal relationships that could have appeared to influence the work reported in this paper.

References

Allsop, D. (2006). *Department of Natural Resources Survey of Tidal Limits and Mangrove Limits in NSW Estuaries 1996 to 2005* (MHL1286). Retrieved from https://www.environment.nsw.gov.au/-/media/OEH/Corporate-Site/Documents/Water/Estuaries/survey-of-tidal-limits-and-mangrove-limits-in-nsw-estuaries-1996-2005.pdf

ASCE. (1992). *Design and construction of urban stormwater management systems*: Reston, Va. : American Society of Civil Engineers.

Award, U. (1995). Environmental Impact Assessment of the Reclamation Project in Isahaya Bay, Nagasaki, Japan. *Journal of Irrigation Engineering and Rural Planning, 1995*(28), 70-73.

Barbosa, A. E., Fernandes, J. N., & David, L. M. (2012). Key issues for sustainable urban stormwater management. *Water Research, 46*(20), 6787-6798. doi:https://doi.org/10.1016/j.watres.2012.05.029

Bosello, F., & De Cian, E. (2014). Climate change, sea level rise, and coastal disasters. A review of modeling practices. *Energy Economics, 46*, 593-605. doi:https://doi.org/10.1016/j.eneco.2013.09.002

Boys, C. A., Kroon, F. J., Glasby, T. M., & Wilkinson, K. (2012). Improved fish and crustacean passage in tidal creeks following floodgate remediation. *Journal of Applied Ecology, 49*(1), 223-233. doi:https://doi.org/10.1111/j.1365-2664.2011.02101.x

Cai, H., Savenije, H. H. G., Garel, E., Zhang, X., Guo, L., Zhang, M., . . . Yang, Q. (2019). Seasonal behaviour of tidal damping and residual water level slope in the Yangtze River estuary: identifying the critical position and river discharge for maximum tidal damping. *Hydrol. Earth Syst. Sci., 23*(6), 2779-2794. doi:10.5194/hess-23-2779-2019

Cavazza, L., & Pisa, P. R. (1988). Effect of watertable depth and waterlogging on crop yield. *Agricultural Water Management, 14*(1), 29-34. doi:https://doi.org/10.1016/0378-3774(88)90057-1

Chant, R. J., Sommerfield, C. K., & Talke, S. A. (2018). Impact of channel deepening on tidal and gravitational circulation in a highly engineered estuarine basin. *Estuaries and Coasts, 41*(6), 1587-1600.

Choi, Y. R. (2014). Modernization, Development and Underdevelopment: Reclamation of Korean tidal flats, 1950s–2000s. *Ocean & coastal management, 102*, 426-436. doi:https://doi.org/10.1016/j.ocecoaman.2014.09.023

Church, J. A., Woodworth, P. L., Aarup, T., & Wilson, W. S. (2010). *Understanding Sea-Level Rise and Variability*.

Couriel, E., Alley, K., & Modra, B. (2012). OEH NSW Tidal Planes Analysis 1990–2010 Harmonic Analysis (Report MHL2053). *Sydney, Australia*.

Dawson, Q., Kechavarzi, C., Leeds-Harrison, P. B., & Burton, R. G. O. (2010). Subsidence and degradation of agricultural peatlands in the Fenlands of Norfolk, UK. *Geoderma, 154*(3), 181-187. doi:https://doi.org/10.1016/j.geoderma.2009.09.017

Day, J. W., & Templet, P. (1989). Consequences of sea level rise: implications from the Mississippi Delta. *Coastal Management, 17*(3), 241-257.

Díez-Minguito, M., Baquerizo, A., Ortega-Sánchez, M., Navarro, G., & Losada, M. (2012). Tide transformation in the Guadalquivir estuary (SW Spain) and process-based zonation. *Journal of Geophysical Research: Oceans, 117*(C3).

Domingues, R. B., Santos, M. C., de Jesus, S. N., & Ferreira, Ó. (2018). How a coastal community looks at coastal hazards and risks in a vulnerable barrier island system (Faro Beach, southern Portugal). *Ocean & coastal management, 157*, 248-256. doi:https://doi.org/10.1016/j.ocecoaman.2018.03.015

Du, J., Shen, J., Zhang, Y. J., Ye, F., Liu, Z., Wang, Z., . . . Wang, H. V. (2018). Tidal Response to Sea-Level Rise in Different Types of Estuaries: The Importance of Length, Bathymetry, and Geometry. *Geophysical Research Letters, 45*(1), 227-235. doi:10.1002/2017gl075963

Dykstra, S. L., Dzwonkowski, B., & Torres, R. (2022). The Role of River Discharge and Geometric Structure on Diurnal Tidal Dynamics, Alabama, USA. *Journal of Geophysical Research: Oceans, 127*(3), e2021JC018007. doi:https://doi.org/10.1029/2021JC018007

Elmoustafa, A. M. (2017). Evaluation of water intake location suitability using a hydrodynamic approach. *Journal of Applied Water Engineering and Research, 5*(1), 31-39. doi:10.1080/23249676.2015.1118364

Environment NSW. (2020, 29 July 2020). Estuaries of NSW. Retrieved from https://www.environment.nsw.gov.au/topics/water/estuaries/estuaries-of-nsw/

Friedrichs, C. T. (2010). Barotropic tides in channelized estuaries. *Contemporary issues in estuarine physics, 27*, 61.

Friedrichs, C. T., & Aubrey, D. G. (1994). Tidal propagation in strongly convergent channels. *Journal of Geophysical Research: Oceans, 99*(C2), 3321-3336.

Gaffield, S. J., Goo, R. L., Richards, L. A., & Jackson, R. J. (2003). Public Health Effects of Inadequately Managed Stormwater Runoff. *American Journal of Public Health, 93*(9), 1527-1533. doi:10.2105/ajph.93.9.1527

Gallo, M. N., & Vinzon, S. B. (2005). Generation of overtides and compound tides in Amazon estuary. *Ocean Dynamics, 55*(5), 441-448.

Geoscience Australia. (2020). Elvis - Elevation and Depth - Foundation Spatial Data. Retrieved from https://elevation.fsdf.org.au/

Giannico, G., & Souder, J. (2004). The Effects of Tide Gates on Estuarine Habitats and Migratory Fish The Effects of Tide Gates on Estuarine Habitats and Migratory Fish. *Oregon Sea Grant*.

Glamore, W. C., Rahman, P., Cox, R., Church, J. & Monselesan, D. (2016). *Sea Level Rise Science and Synthesis for NSW*. Retrieved from

Godin, G. (1985). Modification of river tides by the discharge. *Journal of waterway, port, coastal, and ocean engineering, 111*(2), 257-274.

Gulliver, A., Carnell, P. E., Trevathan-Tackett, S. M., Duarte de Paula Costa, M., Masqué, P., & Macreadie, P. I. (2020). Estimating the Potential Blue Carbon Gains From Tidal Marsh Rehabilitation: A Case Study From South Eastern Australia. *Frontiers in Marine Science, 7*(403). doi:10.3389/fmars.2020.00403

Guo, L., van der Wegen, M., Jay, D. A., Matte, P., Wang, Z. B., Roelvink, D., & He, Q. (2015). River-tide dynamics: Exploration of nonstationary and nonlinear tidal behavior in the Yangtze River estuary. *Journal of Geophysical Research: Oceans, 120*(5), 3499-3521. doi:https://doi.org/10.1002/2014JC010491

Guo, L., Wang, Z. B., Townend, I., & He, Q. (2019). Quantification of Tidal Asymmetry and Its Nonstationary Variations. *Journal of Geophysical Research: Oceans, 124*(1), 773-787. doi:https://doi.org/10.1029/2018JC014372

Guo, W., Wang, X. H., Ding, P., Ge, J., & Song, D. (2018). A system shift in tidal choking due to the construction of Yangshan Harbour, Shanghai, China. *Estuarine, Coastal and Shelf Science, 206*, 49-60. doi:https://doi.org/10.1016/j.ecss.2017.03.017

Hague, B. S., McGregor, S., Murphy, B. F., Reef, R., & Jones, D. A. (2020). Sea Level Rise Driving Increasingly Predictable Coastal Inundation in Sydney, Australia. *Earth's Future, 8*(9). doi:10.1029/2020EF001607

Hague, B. S., & Taylor, A. J. (2021). Tide-only inundation: a metric to quantify the contribution of tides to coastal inundation under sea-level rise. *Natural Hazards, 107*(1), 675-695. doi:10.1007/s11069-021-04600-4

Haigh, I. D., Pickering, M. D., Green, J. A. M., Arbic, B. K., Arns, A., Dangendorf, S., . . . Woodworth, P. L. (2020). The Tides They Are A-Changin': A Comprehensive Review of Past and Future Nonastronomical Changes in Tides, Their Driving Mechanisms, and Future Implications. *Reviews of Geophysics, 58*(1), e2018RG000636. doi:10.1029/2018rg000636

Hanslow, D. J., Fitzhenry, M. G., Power, H. E., Kinsela, M. A., & Hughes, M. G. (2019). *Rising tides: Tidal inundation in south East Australian estuaries.* Paper presented at the Australasian

Coasts and Ports 2019 Conference: Future directions from 40 [degrees] S and beyond, Hobart, 10-13 September 2019.

Harrison, A. J., Rayner, D. S., Tucker, T. A., Lumiatti, G., Rahman, P. F., Glamore, W. C. (2022a). *Clarence River Floodplain Prioritisation Study - Appendix I - Hydrodynamic modelling* (WRL TR 2020/06). Retrieved from Sydney: https://doi.org/10.13140/RG.2.2.31776.05124

Harrison, A. J., Rayner, D. S., Tucker, T. A., Lumiatti, G., Rahman, P. F., Glamore, W. C. (2022b). *Hastings River Floodplain Prioritisation Study - Appendix I - Hydrodynamic modelling* (WRL TR 2020/08). Retrieved from Sydney: https://doi.org/10.13140/RG.2.2.18354.27844

Helaire, L. T., Talke, S. A., Jay, D. A., & Chang, H. (2020). Present and Future Flood Hazard in the Lower Columbia River Estuary: Changing Flood Hazards in the Portland-Vancouver Metropolitan Area. *Journal of Geophysical Research: Oceans, 125*(7), e2019JC015928. doi:https://doi.org/10.1029/2019JC015928

Hino, M., Belanger, S. T., Field, C. B., Davies, A. R., & Mach, K. J. (2019). High-tide flooding disrupts local economic activity. *Science Advances, 5*(2), eaau2736. doi:10.1126/sciadv.aau2736

Hoeksema, R. J. (2007). Three stages in the history of land reclamation in the Netherlands. *Irrigation and Drainage: The Journal of the International Commission on Irrigation and Drainage, 56*(S1), S113-S126.

Holleman, R. C., & Stacey, M. T. (2014). Coupling of Sea Level Rise, Tidal Amplification, and Inundation. *Journal of Physical Oceanography, 44*(5), 1439-1455. doi:10.1175/jpo-d-13-0214.1

Hoover, D. J., Odigie, K. O., Swarzenski, P. W., & Barnard, P. (2017). Sea-level rise and coastal groundwater inundation and shoaling at select sites in California, USA. *Journal of Hydrology: Regional Studies, 11*, 234-249. doi:https://doi.org/10.1016/j.ejrh.2015.12.055

Horner, R. (1979). The Thames barrier project. *Geographical Journal*, 242-253.

Hottinger, S. (2019). *Effects of entrance conditions on tidal hydrodynamics in idealized prismatic estuaries under sea level rise*. Retrieved from

Hsiao, S.-C., Chiang, W.-S., Jang, J.-H., Wu, H.-L., Lu, W.-S., Chen, W.-B., & Wu, Y.-T. (2021). Flood risk influenced by the compound effect of storm surge and rainfall under climate change for low-lying coastal areas. *Science of The Total Environment, 764*, 144439. doi:https://doi.org/10.1016/j.scitotenv.2020.144439

Huntsman, S. R. (2011). Design and Construction of the Lake Borgne Surge Barrier in Response to Hurricane Katrina. In *Coastal Engineering Practice (2011)* (pp. 117-130).

Hurst, C. A., Thorburn, P. J., Lockington, D., & Bristow, K. L. (2004). Sugarcane water use from shallow water tables: implications for improving irrigation water use efficiency. *Agricultural Water Management, 65*(1), 1-19. doi:https://doi.org/10.1016/S0378-3774(03)00207-5

Jalón-Rojas, I., Sottolichio, A., Hanquiez, V., Fort, A., & Schmidt, S. (2018). To What Extent Multidecadal Changes in Morphology and Fluvial Discharge Impact Tide in a Convergent (Turbid) Tidal River. *Journal of Geophysical Research: Oceans, 123*(5), 3241-3258. doi:https://doi.org/10.1002/2017JC013466

Johnston, S. G., Slavich, P. G., & Hirst, P. (2005). The impact of controlled tidal exchange on drainage water quality in acid sulphate soil backswamps. *Agricultural Water Management, 73*(2), 87-111. doi:https://doi.org/10.1016/j.agwat.2004.10.005

Kane, H. H., Fletcher, C. H., Frazer, L. N., & Barbee, M. M. (2015). Critical elevation levels for flooding due to sea-level rise in Hawaiʻi. *Regional Environmental Change, 15*(8), 1679-1687. doi:10.1007/s10113-014-0725-6

Karegar, M. A., Dixon, T. H., Malservisi, R., Kusche, J., & Engelhart, S. E. (2017). Nuisance Flooding and Relative Sea-Level Rise: the Importance of Present-Day Land Motion. *Scientific reports, 7*(1), 11197. doi:10.1038/s41598-017-11544-y

Khojasteh, D., Chen, S., Felder, S., Heimhuber, V., & Glamore, W. (2021). Estuarine tidal range dynamics under rising sea levels. *PloS one, 16*(9), e0257538.

Khojasteh, D., Glamore, W., Heimhuber, V., & Felder, S. (2021). Sea level rise impacts on estuarine dynamics: A review. *Science of The Total Environment, 780*, 146470. doi:https://doi.org/10.1016/j.scitotenv.2021.146470

King, I. P. (2015). *RMA2 – A Two Dimensional Finite Element Model For Flow in Estuaries and Streams*. Sydney Australia: Resource Modelling Associates.

Kroon, F. J., & Ansell, D. H. (2006). A comparison of species assemblages between drainage systems with and without floodgates: implications for coastal floodplain management. *Canadian Journal of Fisheries and Aquatic Sciences, 63*(11), 2400-2417.

Kulp, S. A., & Strauss, B. H. (2019). New elevation data triple estimates of global vulnerability to sea-level rise and coastal flooding. *Nature Communications, 10*(1), 4844. doi:10.1038/s41467-019-12808-z

Lang, T. A., Oladeji, O., Josan, M., & Daroub, S. (2010). Environmental and management factors that influence drainage water P loads from Everglades Agricultural Area farms of South Florida. *Agriculture, Ecosystems & Environment, 138*(3), 170-180. doi:https://doi.org/10.1016/j.agee.2010.04.015

Lee, S. B., Li, M., & Zhang, F. (2017). Impact of sea level rise on tidal range in Chesapeake and Delaware Bays. *Journal of Geophysical Research: Oceans, 122*(5), 3917-3938. doi:https://doi.org/10.1002/2016JC012597

Lugo, A. E., & Snedaker, S. C. (1974). The Ecology of Mangroves. *5*(1), 39-64. doi:10.1146/annurev.es.05.110174.000351

Magnan, A. K., Garschagen, M., Gattuso, J.-P., Hay, J. E., Hilmi, N., Holland, E., . . . Petzold, J. (2019). Cross-chapter box 9: integrative cross-chapter box on low-lying islands and coasts. In *IPCC Special Report on the Ocean and Cryosphere in a Changing Climate* (pp. 657-674).

Manda, A. K., Owers, J. E., Jr., & Allen, T. (2017). Simulating marine and groundwater inundation on a barrier island setting under changing sea-level rise scenarios. In (Vol. 49). Boulder, CO: Boulder, CO, United States: Geological Society of America (GSA).

Marfai, M. A., & King, L. (2008). Potential vulnerability implications of coastal inundation due to sea level rise for the coastal zone of Semarang city, Indonesia. *Environmental Geology, 54*(6), 1235-1245. doi:10.1007/s00254-007-0906-4

Martínez, M. L., Intralawan, A., Vázquez, G., Pérez-Maqueo, O., Sutton, P., & Landgrave, R. (2007). The coasts of our world: Ecological, economic and social importance. *Ecological Economics, 63*(2), 254-272. doi:https://doi.org/10.1016/j.ecolecon.2006.10.022

Masson-Delmotte, V., Zhai, P., Priani, A., Connors, S. L., Pean, C., Berger, S., . . . Zhou, B. (2021). *IPCC: Climate Change 2021: The Physical Science Basis. Contribution of Working Group I to the Sixth Assessment Report of the Intergovernmental Panel on Climate Change.* Retrieved from

Moftakhari, H. R., AghaKouchak, A., Sanders, B. F., Allaire, M., & Matthew, R. A. (2018). What Is Nuisance Flooding? Defining and Monitoring an Emerging Challenge. *Water Resources Research, 54*(7), 4218-4227. doi:https://doi.org/10.1029/2018WR022828

Neumann B, V. A., Zimmermann J, Nicholls RJ. (2015). Future Coastal Population Growth and Exposure to Sea-Level Rise and Coastal Flooding-A Global Assessment. *PloS one, 10*(3), e0118571. Retrieved from https://doi.org/10.1371/journal.pone.0118571

Nicholls, R. J. (2015). Chapter 9 - Adapting to Sea Level Rise. In J. F. Shroder, J. T. Ellis, & D. J. Sherman (Eds.), *Coastal and Marine Hazards, Risks, and Disasters* (pp. 243-270). Boston: Elsevier.

Nidzieko, N. J. (2010). Tidal asymmetry in estuaries with mixed semidiurnal/diurnal tides. *Journal of Geophysical Research: Oceans, 115*(C8). doi:https://doi.org/10.1029/2009JC005864

Ohle, N., Schuster, D., Kappenberg, J., Sothmann, J., & Rudolph, E. (2017). Artificial sandbanks in the Elbe Estuary mouth: a method for surge mitigation? *Journal of Applied Water Engineering and Research, 5*(2), 158-166. doi:10.1080/23249676.2016.1184596

Oliver-Smith, A. (2009). *Sea level rise and the vulnerability of coastal peoples: responding to the local challenges of global climate change in the 21st century*: UNU-EHS.

Orton, P. M., Conticello, F. R., Cioffi, F., Hall, T. M., Georgas, N., Lall, U., . . . MacManus, K. (2020). Flood hazard assessment from storm tides, rain and sea level rise for a tidal river estuary. *Natural Hazards, 102*(2), 729-757. doi:10.1007/s11069-018-3251-x

Orton, P. M., Talke, S. A., Jay, D. A., Yin, L., Blumberg, A. F., Georgas, N., . . . MacManus, K. (2015). Channel Shallowing as Mitigation of Coastal Flooding. *Journal of Marine Science and Engineering, 3*(3), 654-673. Retrieved from https://www.mdpi.com/2077-1312/3/3/654

Ota, S. (2018). Key Factors in Handling Conflicts in the Isahaya Bay Land Reclamation Project, Japan: A Case Study Focusing on Social Aspects. *Irrigation and Drainage, 67*(S1), 96-104. doi:https://doi.org/10.1002/ird.2202

Pachauri, R. K., Allen, M. R., Barros, V. R., Broome, J., Cramer, W., Christ, R., . . . Dasgupta, P. (2014). *Climate change 2014: synthesis report. Contribution of Working Groups I, II and III to the fifth assessment report of the Intergovernmental Panel on Climate Change*: Ipcc.

Poulter, B., Goodall, J. L., & Halpin, P. N. (2008). Applications of network analysis for adaptive management of artificial drainage systems in landscapes vulnerable to sea level rise. *Journal of Hydrology, 357*(3), 207-217. doi:https://doi.org/10.1016/j.jhydrol.2008.05.022

Proudfoot, M., Valentine, E. M., Evans, K. G., & King, I. (2018). Calibration of a Marsh-Porosity Finite Element Model: Case Study from a Macrotidal Creek and Floodplain in Northern Australia. *Journal of Hydraulic Engineering, 144*(2), 05017005.

Raw, J. L., Adams, J. B., Bornman, T. G., Riddin, T., & Vanderklift, M. A. (2021). Vulnerability to sea-level rise and the potential for restoration to enhance blue carbon storage in salt marshes of an urban estuary. *Estuarine, Coastal and Shelf Science, 260*, 107495. doi:https://doi.org/10.1016/j.ecss.2021.107495

Rillahan, C. B., Alcott, D., Castro-Santos, T., & He, P. (2021). Activity Patterns of Anadromous Fish below a Tide Gate: Observations from High-Resolution Imaging Sonar. *Marine and Coastal Fisheries, 13*(3), 200-212. doi:https://doi.org/10.1002/mcf2.10149

Ruprecht, J., Glamore, W., & Rayner, D. (2018). Estuarine dynamics and acid sulfate soil discharge: Quantifying a conceptual model. *Ecological Engineering, 110*, 172-184.

Sheehan, L., Sherwood, E. T., Moyer, R. P., Radabaugh, K. R., & Simpson, S. (2019). Blue Carbon: an Additional Driver for Restoring and Preserving Ecological Services of Coastal Wetlands in Tampa Bay (Florida, USA). *Wetlands, 39*(6), 1317-1328. doi:10.1007/s13157-019-01137-y

Smolders, S., João Teles, M., Leroy, A., Maximova, T., Meire, P., & Temmerman, S. (2020). Modeling Storm Surge Attenuation by an Integrated Nature-Based and Engineered Flood Defense System in the Scheldt Estuary (Belgium). *Journal of Marine Science and Engineering, 8*(1), 27. Retrieved from https://www.mdpi.com/2077-1312/8/1/27

Solomon, D. (2010). Eel passage at tidal structures and pumping stations. *Commisioned by: Environment Agency, Thames Region. Foundry Farm, Kiln Lane, Redlynch, Salisbury, Wilts, SP5 2HT. Final Report*.

Song, D., Wang, X. H., Kiss, A. E., & Bao, X. (2011). The contribution to tidal asymmetry by different combinations of tidal constituents. *Journal of Geophysical Research: Oceans, 116*(C12). doi:https://doi.org/10.1029/2011JC007270

Stark, J., Plancke, Y., Ides, S., Meire, P., & Temmerman, S. (2016). Coastal flood protection by a combined nature-based and engineering approach: Modeling the effects of marsh geometry and surrounding dikes. *Estuarine, Coastal and Shelf Science, 175*, 34-45. doi:https://doi.org/10.1016/j.ecss.2016.03.027

Talke, S. A., & Jay, D. A. (2020). Changing Tides: The Role of Natural and Anthropogenic Factors. *Annual Review of Marine Science, 12*(1), 121-151. doi:10.1146/annurev-marine-010419-010727

Titus, J. G., Hudgens, D. E., Trescott, D. L., Craghan, M., Nuckols, W. H., Hershner, C. H., . . . Wang, J. (2009). State and local governments plan for development of most land vulnerable to rising sea level along the US Atlantic coast. *Environmental Research Letters, 4*(4), 044008. doi:10.1088/1748-9326/4/4/044008

Titus, J. G., Kuo, C. Y., Gibbs, M. J., LaRoche, T. B., Webb, M. K., & Waddell, J. O. (1987). Greenhouse effect, sea level rise, and coastal drainage systems. *Journal of Water Resources Planning and Management, 113*(2), 216-227.

Tulau, M. J. (2011). Lands of the richest character: Agricultural drainage of backswamp wetlands on the north coast of New South Wales, Australia: Development, conservation and policy change: An environmental history.

van Rijn, L. C. (2011). Analytical and numerical analysis of tides and salinities in estuaries; part I: tidal wave propagation in convergent estuaries. *Ocean Dynamics, 61*(11), 1719-1741.

Vitousek, S., Barnard, P. L., Fletcher, C. H., Frazer, N., Erikson, L., & Storlazzi, C. D. (2017). Doubling of coastal flooding frequency within decades due to sea-level rise. *Scientific reports, 7*(1). doi:10.1038/s41598-017-01362-7

Vlotman, W. F., Smedema, L. K., & Rycroft, D. W. (2020). *Modern land drainage: Planning, design and management of agricultural drainage systems*: CRC Press.

von Storch, H., Gönnert, G., & Meine, M. (2008). Storm surges—An option for Hamburg, Germany, to mitigate expected future aggravation of risk. *Environmental Science & Policy, 11*(8), 735-742. doi:https://doi.org/10.1016/j.envsci.2008.08.003

Waddington, K., Khojasteh, D., Marshall, L., Rayner, D., Glamore, W. (2022). *Quantifying the Effects of Sea Level Rise on Estuarine Drainage Systems [Dataset]*. Retrieved from: https://doi.org/10.13140/RG.2.2.28047.87208

Wahyudi, S. I., Adi, H. P., Lekerkerk, J., Bakker, L., Ven, M., & Vermeer, D. (2019). Assessment of polder system drainage experimentation performance related to tidal floods in Mulyorejo, Pekalongan, Indonesia. *Int. J. Integr. Eng., 9*, 73-82.

Wake, C. P., Knott, J., Lippmann, T., Stampone, M. D., Ballestero, T. P., Bjerklle, D., . . . Jacobs, J. M. (2019). New Hampshire Coastal Flood Risk Summary Part 1: Science.

Warner, J. F., van Staveren, M. F., & van Tatenhove, J. (2018). Cutting dikes, cutting ties? Reintroducing flood dynamics in coastal polders in Bangladesh and the netherlands. *International Journal of Disaster Risk Reduction, 32*, 106-112. doi:https://doi.org/10.1016/j.ijdrr.2018.03.020

White, N. J., Haigh, I. D., Church, J. A., Koen, T., Watson, C. S., Pritchard, T. R., . . . You, Z.-J. (2014). Australian sea levels—Trends, regional variability and influencing factors. *Earth-Science Reviews, 136*, 155-174.

Williams, R. J., & Watford, F. A. (1997). Identification of structures restricting tidal flow in New South Wales, Australia. *Wetlands Ecology and Management, 5*(1), 87-97. doi:10.1023/A:1008283522167

Xu, G., & Blussé, L. (2019). Land Reclamation in the Rhine and Yangzi Deltas: An Explorative Comparison, 1600–1800. *Fudan Journal of the Humanities and Social Sciences, 12*(3), 423-455. doi:10.1007/s40647-018-0223-1

Yang, X. (2008). Evaluation and application of DRAINMOD in an Australian sugarcane field. *Agricultural Water Management, 95*(4), 439-446. doi:https://doi.org/10.1016/j.agwat.2007.11.006

Zhang, M., Dai, Z., Bouma, T. J., Bricker, J., Townend, I., Wen, J., . . . Cai, H. (2021). Tidal-flat reclamation aggravates potential risk from storm impacts. *Coastal Engineering, 166*, 103868. doi:https://doi.org/10.1016/j.coastaleng.2021.103868

Zhang, W., Cao, Y., Zhu, Y., Zheng, J., Ji, X., Xu, Y., . . . Hoitink, A. (2018). Unravelling the causes of tidal asymmetry in deltas. *Journal of Hydrology, 564*, 588-604.

Zhao, C., Yang, H., Zhongya, F., Zhu, L., Wang, W., & Zeng, F. (2020). Impacts of Tide Gate Modulation on Ammonia Transport in a Semi-closed Estuary during the Dry Season—A Case Study at the Lianjiang River in South China. *Water, 12*, 1945. doi:10.3390/w12071945